THE GEOLOGICAL SOCIETY OF AMERICA®

A new K-Ar illite dating application to constrain the timing of subduction in West Sarawak, Borneo

Qi Zhao[1,2,4], Yi Yan[1,2,3,5,†], Satoshi Tonai[6], Naotaka Tomioka[7], Peter D. Clift[8,9], Meor H. Amir Hassan[10], and Jasmi Hafiz Bin Abdul Aziz[10]

[1]*Key Laboratory of Ocean and Marginal Sea Geology, Guangzhou Institute of Geochemistry, Chinese Academy of Sciences, Guangzhou 510640, China*
[2]*CAS Center for Excellence in Deep Earth Science, Guangzhou 510640, China*
[3]*Southern Marine Science and Engineering Guangdong Laboratory (Guangzhou) 511458, China*
[4]*College of Earth and Planetary Sciences, University of Chinese Academy of Sciences, Beijing 100049, China*
[5]*Innovation Academy of South China Sea Ecology and Environmental Engineering, Chinese Academy of Sciences, Guangzhou 511458, China*
[6]*Faculty of Science and Technology, Kochi University, Kochi 780-8520, Japan*
[7]*Kochi Institute for Core Sample Research, Japan Agency for Marine-Earth Science and Technology, Kochi 783-8502, Japan*
[8]*Department of Geology and Geophysics, E235 Howe-Russell-Kniffen Geoscience Complex Louisiana State University, Baton Rouge, Louisiana 70803, USA*
[9]*Research Center for Earth System Science, Yunnan University, Kunming, Yunnan, China*
[10]*Department of Geology, University of Malaya, 50603 Kuala Lumpur, Malaysia*

ABSTRACT

The timing of subduction is a fundamental tectonic problem for tectonic models, yet there are few direct geological proxies for constraining it. However, the matrix of a tectonic mélange formed in a subduction-accretion setting archives the physical/chemical attributes at the time of deformation during the subduction-accretion process. Thus, the deformation age of the matrix offers the possibility to directly constrain the period of the subduction-accretion process. Here we date the Lubok Antu tectonic mélange and the overlying Lupar Formation in West Sarawak, Borneo by K-Ar analysis of illite. The ages of authigenic illite cluster around 60 Ma and 36 Ma. The maximum temperatures calculated by vitrinite reflectance values suggest that our dating results were not affected by external heating. Thus, the ages of authigenic illite represent the deformation age of the mélange matrix and the timing of the Rajang Unconformity, indicating that the subduction in Sarawak could have continued until ca. 60 Ma and the thermal and/or fluid flow events triggered by a major uplift of the Rajang Group occurred at ca. 36 Ma. Furthermore, this study highlights the potential of using the tectonic mélange to extract the timeframe of subduction zone episodic evolution directly.

INTRODUCTION

The timing of subduction may be determined by constraining the timing of arc volcanism, forearc-backarc faulting, and high-temperature metamorphic soles. However, magma formation, melt transport, and emplacement result in an unknown lag compared to the timing of subduction (Domeier et al., 2018). Ophiolites preserved in forearcs and the high-temperature metamorphic soles that directly record the initiation of subduction are often deeply buried, especially in active systems (Stern et al., 2012). Sometimes, in areas with complex tectonic histories, such as Borneo, an island which was assembled from different fragments during the Cretaceous (Figs. 1A and 1B; Hall, 2012), the subduction-related magmatism is difficult to match with the exact active subduction zone. For example, Hall (2012) suggested that the magmatic rocks (ca. 130 Ma–85 Ma) of the Schwaner Mountains in Southwest Borneo are the result of south-directed subduction beneath the SW Borneo block as it moved north from the Australian margin of Gondwana by the Late Jurassic. Breitfeld et al. (2017) and Hennig et al. (2017) argued that the magmatic rocks of the Schwaner Mountains record Cretaceous magmatism at the paleo-Pacific subduction margin (Figs. 1A and 1B). This lack of direct geologic constraints on the timing of subduction remains a significant gap in our understanding of the tectonic history and lifecycle of subduction.

Mélanges are block-in-matrix units that form by tectonic, sedimentary, and diapiric processes in subduction-accretion complexes and orogenic belts (Festa et al., 2010, 2019; Raymond, 2019). The geodynamic environment of the tectonic mélange formed in a subduction-accretion setting can be divided into two sections: (1) the front of the wedge and (2) the base of the wedge and subduction channel (Festa et al., 2012, 2019; Raimbourg et al., 2019; Raymond, 2019; Fig. 2). These mélanges facilitate preservation of inter-mélange, less deformed, accretionary units (Raymond, 2019). Offscraped tectonic mélange associated with shear/fault zones in the front of the wedge result in the mixing and/or juxtaposition of coherent units during the development of the accretionary complex (Fig. 2; Festa et al., 2019; Raymond, 2019). Tectonic mélange formed along the plate interface is suggested to be a fossil plate boundary based on the fault-related chaotic character (Fig. 2; Fagereng and Sibson, 2010; Kimura et al., 2012; Kitamura et al., 2005). The matrix of the tectonic mélange generally deforms by pressure-solution accommodated frictional slip during mélange lithification and deformation in the subduction-accretion process (Fagereng and Den Hartog, 2017). Hence, the matrix of a tectonic mélange could archive the physical/chemical attributes (e.g., characteristic deformation structures,

Yi Yan https://orcid.org/0000-0003-2475-6817
†Corresponding author: yanyi@gig.ac.cn.

GSA Bulletin; January/February 2022; v. 134; no. 1/2; p. 405–418; https://doi.org/10.1130/B35895.1; 9 figures; 2 tables; 1 supplemental file.
published online 17 May 2021

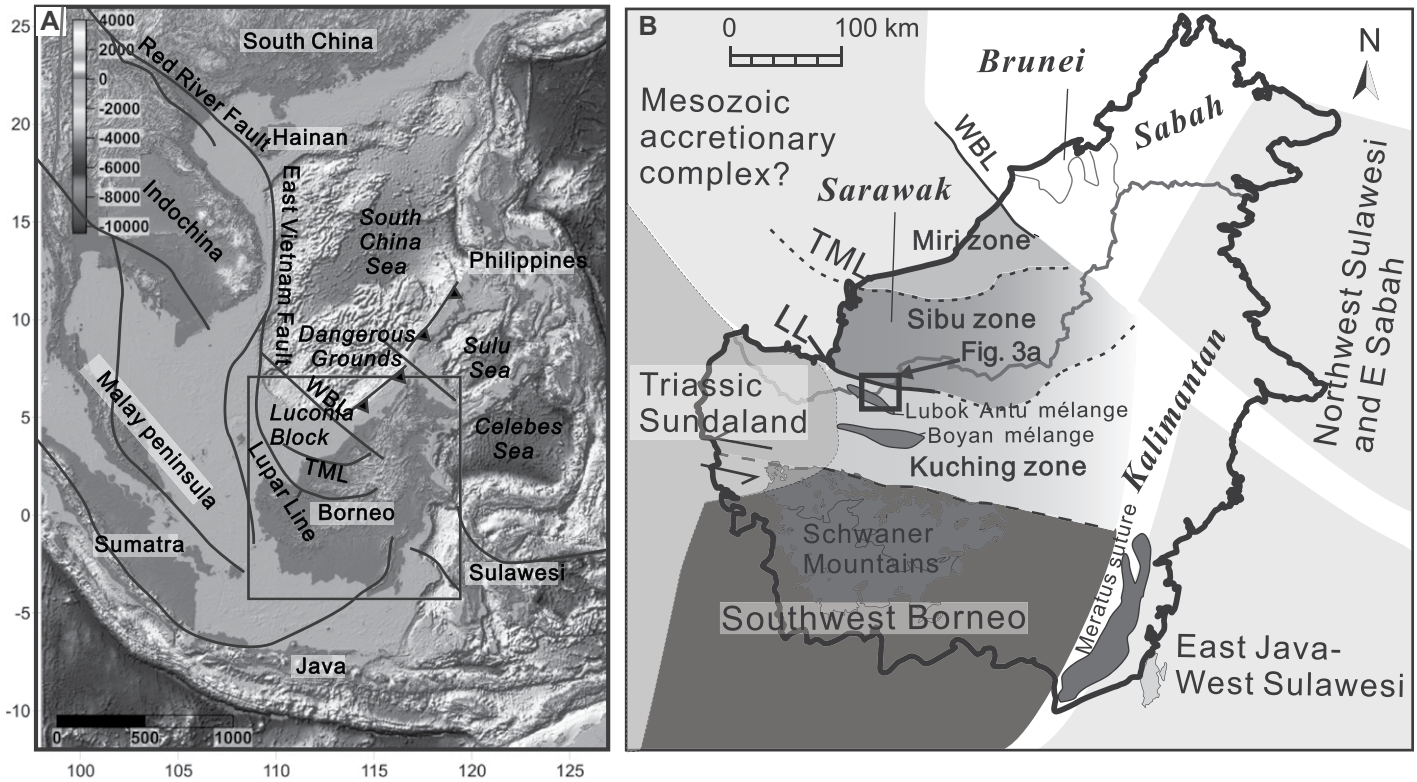

Figure 1. Overview and sample map of the study area. (A) Simplified map of regional tectonic characteristics of Borneo (modified from Wang et al., 2016). LL—Lupar Line; TML—Tatau Mersing Line; WBL—West Balam Line. (B) Tectonic provinces of Borneo (basement map, after Breitfeld et al., 2017) and four sub-parallel structural terranes of Borneo (after Haile, 1974).

authigenic/synkinematic illite) at the time of deformation in a subduction-accretion setting, and offers the possibility to constrain the time of the subduction-accretion process.

The Lubok Antu Mélange formed in a subduction-accretion setting is exposed along the Lupar Line in Sarawak, Borneo (Breitfeld et al., 2017; Hall and Breitfeld, 2017; Hennig et al., 2017; Hutchison, 2005; Tan, 1979, 1982; Williams et al., 1988; Fig. 1B). However, the formation/deformation age of the Lubok Antu Mélange in West Sarawak has never been

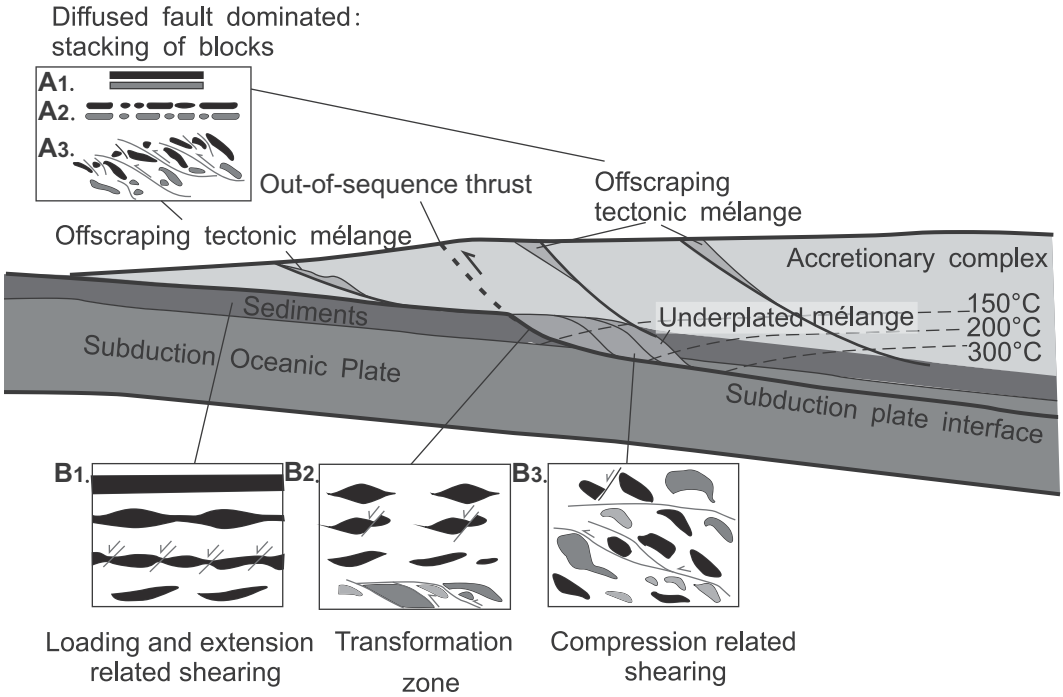

Figure 2. Cartoon showing subduction and tectonic mélange formation. Note the possible location for tectonic mélange formation in subduction-accretion setting: (A_1–A_3) Progressive deformation in the front of the wedge (after Festa et al., 2012); (B_1–B_3) Progressive deformation in the subduction channel (after Festa et al., 2012).

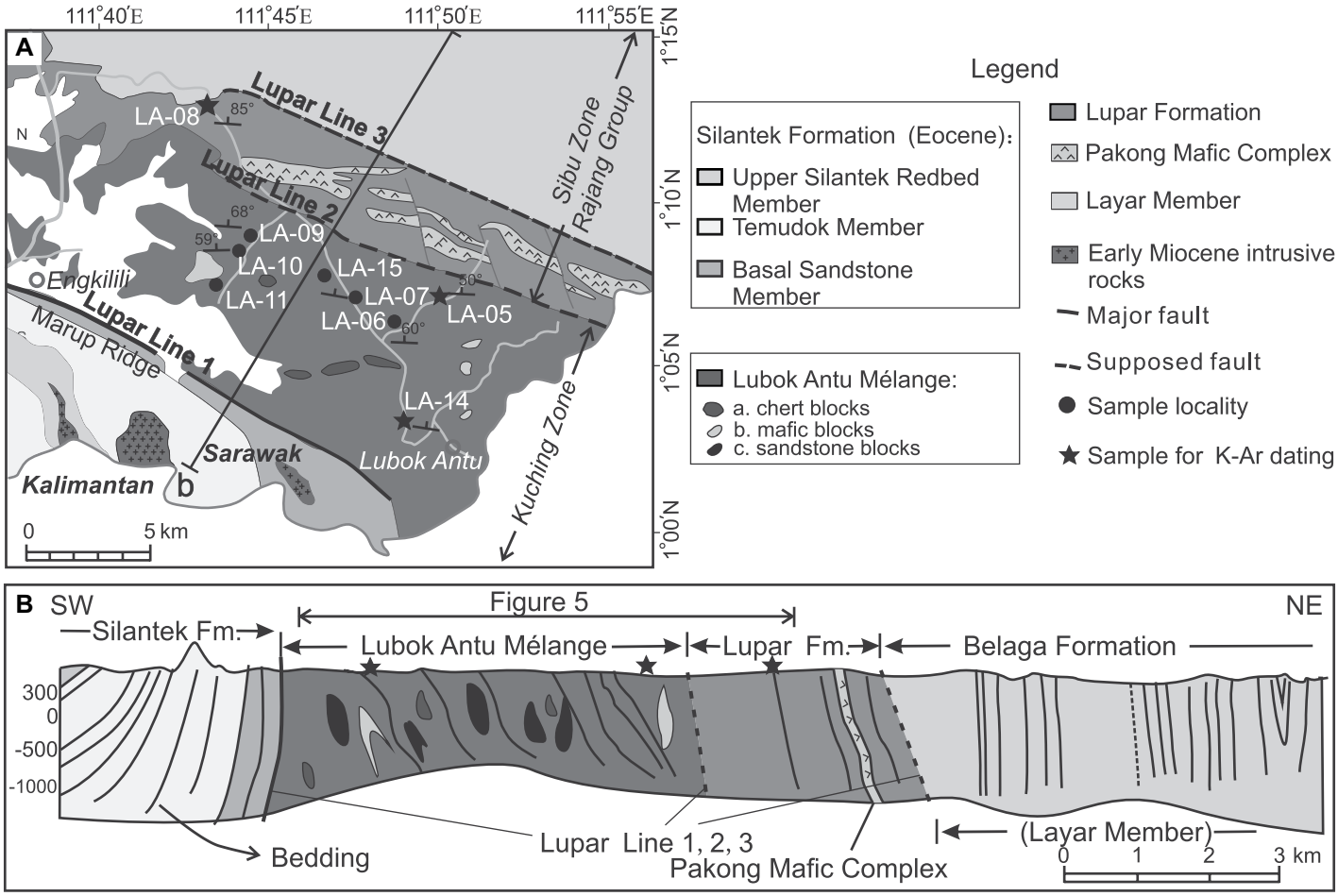

Figure 3. (A) Simplified geological map of Lubok Antu, Sarawak, Borneo after Tan (1982) and Tate (2002). The locations of samples for vitrinite reflectance analysis and K-Ar dating are indicated by circles and stars, respectively. (B) Cross section through Lupar Line (modified from Honza et al., 2000). Fm.—Formation.

determined because of the lack of geological records such as macrofossils and microfossils that can be dated by conventional techniques. The Lupar Line that separates the Sibu Zone from the Kuching Zone to the south was interpreted as a suture (e.g., Hutchison, 1996, 2005, 2010; Tan, 1979, 1982), but could also be a major strike-slip fault which was active during the Cenozoic (e.g., Breitfeld et al., 2017; Haile, 1974; Hall, 2012; Hall and Breitfeld, 2017; Hall and Sevastjanova, 2012; Fig. 1B). The strike-slip fault system, such as the Lupar Line bounding the Lubok Antu Mélange might be related to the counter-clockwise rotation of Borneo (Figs. 3A and 3B; Schmidtke et al., 1990; Fuller et al., 1999). The Lupar Line bounding the mélange could have been reactivated as the locus of shear during post-subduction deformation, thus, the Lubok Antu Mélange may archive the physical/chemical properties of its initial formation/deformation. We therefore attempt to apply the illite age analysis (IAA) approach to the pelitic matrix of the Lubok Antu Mélange and the mudstone of the Lupar Formation to explore the deformation age of the mélange matrix and the diagenetic age of illite from the Lupar Formation, respectively. We also analyze the potential for external heating and consider that our K-Ar analysis provides geologically significant and meaningful ages when applying the conceptual model of the IAA approach. This study provides a constraint on the subduction-accretion process in West Sarawak that is important when considering the tectonic evolution of the South China Sea region and offers a new application of the K-Ar illite dating approach. Dating the formation/deformation age of the tectonic mélange in a subduction-accretion setting may be a direct approach for constraining the timing of subduction.

ILLITE AGE ANALYSIS

It has long been recognized that the abundance of the $2M_1$ illite/muscovite polytype relative to the $1M/1M_d$ illite polytype decreases systematically with grain size (Grathoff et al., 1998; Pevear, 1992) and the K-Ar or Ar-Ar age also decreases systematically with grain size in shales (Clauer et al., 1997; Hower et al., 1963; Velde and Hower, 1963). These paired observations led to the widely accepted interpretation that the $1M/1M_d$ polytype component is authigenic, whereas the $2M_1$ polytype component is detrital (Aldega et al., 2019; Fisher et al., 2019; Grathoff et al., 2001; Hower et al., 1963; Reynolds, 1963; Tonai et al., 2016; Torgersen et al., 2014), although it may also be caused by progressive mineral growth (Meunier et al., 2004) or Ar loss (Verdel et al., 2012). The K-Ar or Ar-Ar age of the finest fraction is considered to be closest to the age of authigenic/synkinematic $1M/1M_d$ illite growth, but it still reflects the contribution of reworked/detrital $2M_1$ illite/muscovite. If the percentage of $2M_1$ polytype illite is linearly related to the age for the different clay size populations, the ages of 100% $1M/1M_d$ polytype and 100% $2M_1$ polytype can be obtained by plotting apparent K-Ar or Ar-Ar age and $2M_1$ polytype

percentage by linear extrapolation of ordinary least square regression (Illite Age Analysis or IAA plot; van der Pluijm et al., 2001). Thus, the net contribution of authigenic/synkinematic $1M/1M_d$ polytype and of $2M_1$ polytype can be determined by the IAA approach.

IAA approach has been used to assess the effects of contamination of potential host rocks when dating diagenesis in sedimentary rocks (e.g., Pevear, 1992, 1999) and motion on shallow faults (e.g., Aldega et al., 2019; Fisher et al., 2019; van der Pluijm et al., 2001, 2006). For the low-temperature fault rocks composed of the detrital $2M_1$ polytype (which is most likely to represent high-temperature illite or muscovite derived from the earlier rock history) and the authigenic $1M/1M_d$ polytype formed during faulting. The extrapolated pure authigenic $1M/1M_d$ illite end member age has been widely accepted as the age of the latest major slip of faulting (e.g., Aldega et al., 2019; Fisher et al., 2019; Haines and van der Pluijm, 2008). The dissolution-precipitation reaction driven by deformation in fault rock is considered to be responsible for the youngest authigenic/synkinematic illite growth (Vrolijk and van der Pluijm, 1999; Vrolijk et al., 2018).

However, the $2M_1$ component clearly does not simply give the original protolithic illite/muscovite age. The $2M_1$ illite/muscovite polytype may represent: (1) authigenic high-temperature illite, (2) cataclastic, synkinematic muscovite from earlier tectonothermal events, (3) detrital muscovite derived from wall-rock, or (4) a mixture of these (Aldega et al., 2019; Carboni et al., 2020; Pevear, 1999; Torgersen et al., 2014). In the same fault zone, it is very common that the extrapolated $2M_1$ illite/muscovite polytype ages (the upper age intercept in the IAA plot) show obvious differences (e.g., Aldega et al., 2019; Song et al., 2014; van der Pluijm et al., 2006). Although van der Pluijm et al. (2006) proposed that the detrital mixtures lead to large variations of the 100% $2M_1$ polytype ages, a linear relationship between K-Ar/Ar-Ar age and percentage of $2M_1$ component is highly unlikely because the $2M_1$ polytypes with different ages are required to have the same relative proportions in all size fractions (Duvall et al., 2011). Thus, if the 100% $2M_1$ polytype shows an older K-Ar or Ar-Ar age than the depositional age of the host rock, the $2M_1$ polytype is suggested to be a detrital illite/muscovite component (e.g., Fisher et al., 2019;van der Pluijm et al., 2001). If the 100% $2M_1$ polytype age is younger than the depositional age of the host rock, the extrapolated $2M_1$ polytype age cannot be considered as a detrital illite/muscovite age of the original protolithic but may represent an authigenic/synkinematic illite/muscovite age during episodes of regional deformation or fluid flow (e.g., Aldega et al., 2019; Song et al., 2014). Thus, the geological significance of the $2M_1$ polytype age should be evaluated carefully in the light of known regional geological events.

Fine-grained clays are mostly susceptible to ^{39}Ar recoil when using the ^{40}Ar-^{39}Ar method for dating (Clauer et al., 2012; Kunk and Brusewitz, 1987). In addition, the step-heating patterns obtained by ^{40}Ar-^{39}Ar method may represent a result of simultaneous degassing of various mineral "Ar reservoirs" in each size fraction, yielding geologically meaningless ages (Clauer et al., 2012; Kula et al., 2010; van der Pluijm et al., 2001). Thus, K-Ar dating method is used for measuring the total gas Ar ages in this study.

GEOLOGICAL SETTING AND SAMPLE DESCRIPTION

Sarawak and West Kalimantan have been divided into four sub-parallel terranes with distinctive geological characteristics and tectonic significances, which, from south to north, are: the Southwest Borneo, mainly composed of Cretaceous magmatic and meta-igneous rocks, the Kuching Zone composed of upper Cretaceous to Cenozoic terrestrial sedimentary rocks, the Sibu Zone made of uppermost Cretaceous–Eocene steeply dipping deep-water turbidite deposits of the Rajang Group, and the Miri Zone comprising post-Eocene undeformed fluvial-shelf sedimentary rocks (Haile, 1974; Figs. 1B and 4).

The Lubok Antu Mélange is found along the Lupar Line, which is the boundary between the deep marine Rajang Group (Sibu Zone) and the terrestrial sedimentary rocks of West Sarawak (Kuching Zone; Fig. 1B) to the south. The mélange strikes west-northwest and dips steeply to the north (Figs. 3A and 3B). Clasts of shale, mudstone, sandstone, limestone, chert, serpentinite, gabbro, and basalt are randomly distributed in its tectonically sheared pelitic matrix (Tan, 1982). Non-coaxial extension and asymmetric fabrics of the sandstone blocks in the Lubok Antu Mélange indicate top-to-north shearing (Figs. 5A–5D). Asymmetric boudin is

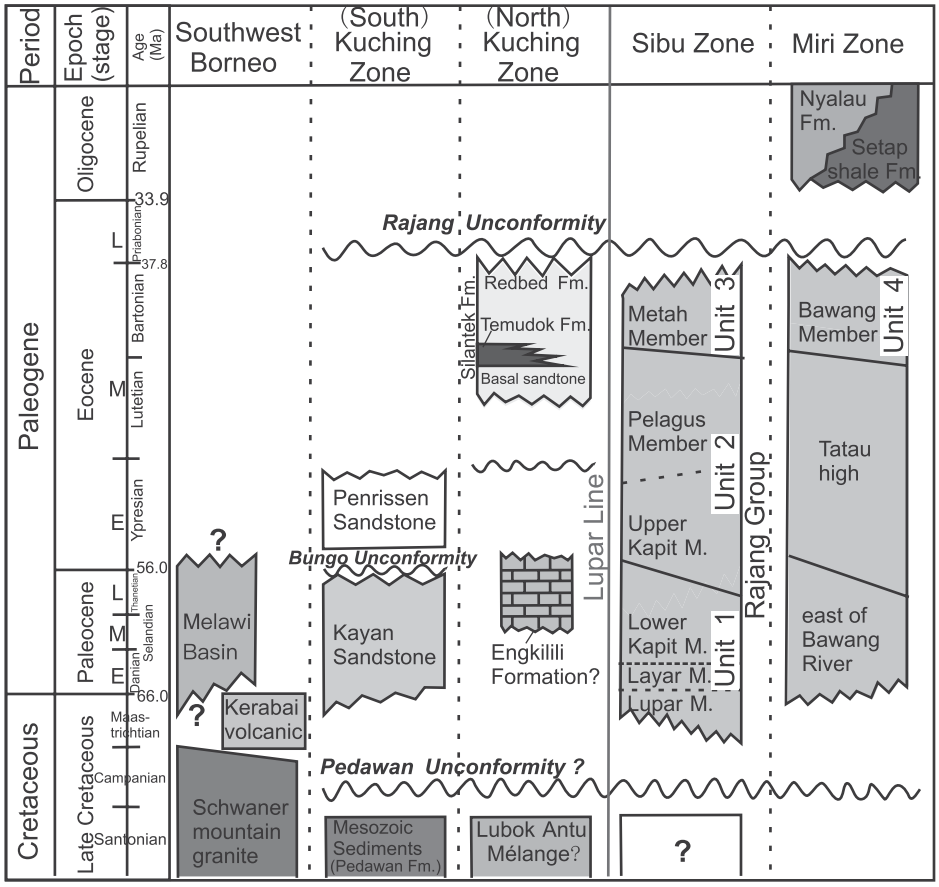

Figure 4. The stratigraphy of four sub-parallel structural terranes of Borneo (after Tan, 1982; Williams et al., 1988; Breitfeld et al., 2018; Galin et al., 2017; Hennig-Breitfeld et al., 2019). The stratigraphic columns of SW Borneo (based on Williams et al., 1988; Doutch, 1992; Breitfeld et al., 2020a). Fm.—Formation; M.—Member.

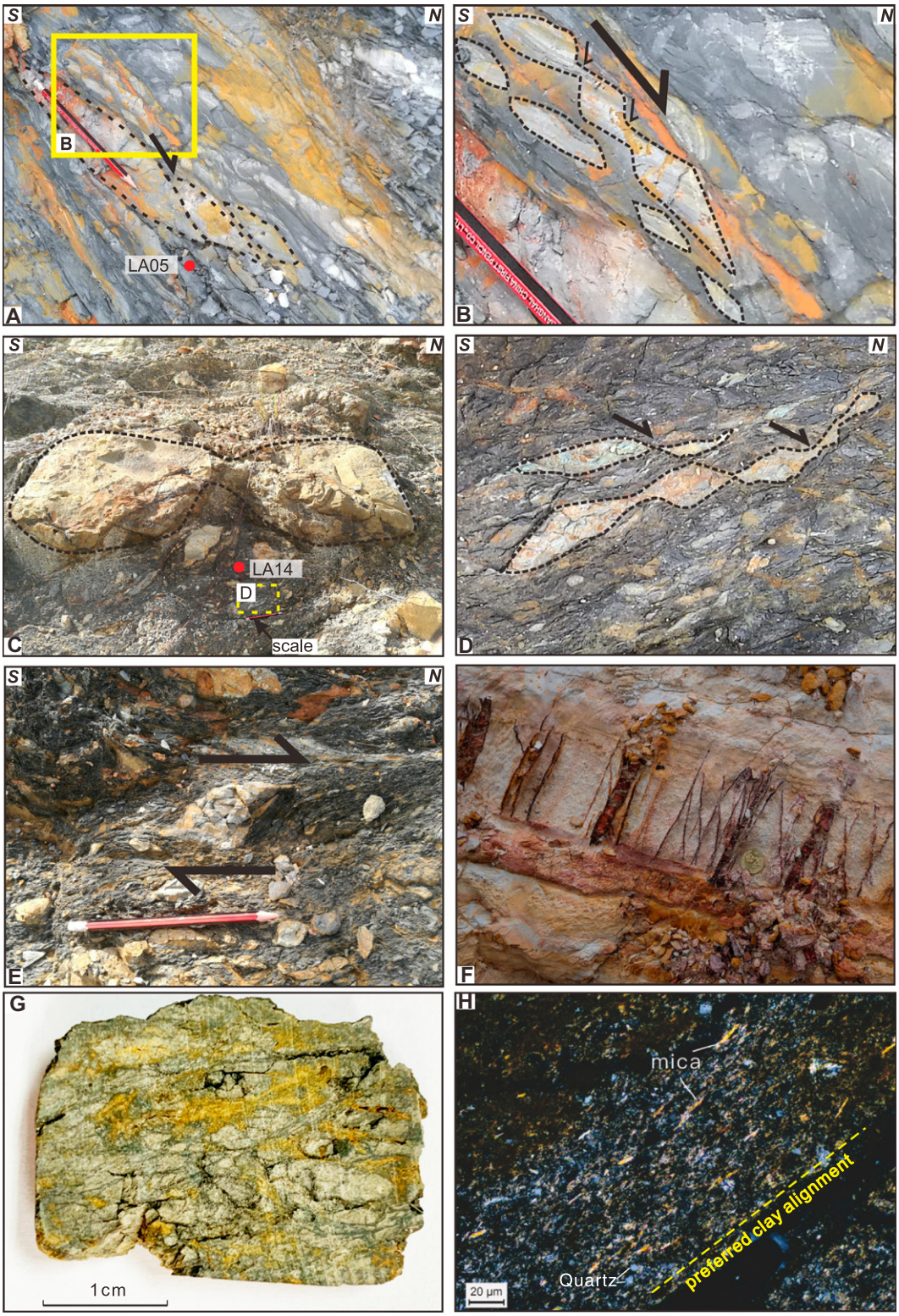

Figure 5. Outcrops and photomicrograph of the Lubok Antu Mélange and the Lupar Formation, Sarawak, Borneo. (A–D) Non-coaxial extension and asymmetric fabrics of sandstone blocks in the Lubok Antu Mélange. (E) Asymmetric flow deformation of the pelitic matrix are observed around sandstone blocks. (F) Outcrops show the coherent Lupar Formation. (G) Photograph of hand specimens: mélange mudstone matrix (LA-14). Note the non-coaxial extension and asymmetric fabrics. (H) Petrographic investigations using optical microscopy for sample LA-14. Note distinct, strongly preferred alignment of clay minerals from lower-left to upper-right. Such fabrics often associated with shear zones in clay-rich rocks help confirm the pre- to syn-tectonic origin of clay minerals.

surrounded by pelitic matrix which flows ductilely, indicating deformation by dissolution-precipitation creep as the rocks lithified (Fig. 5E; e.g., Fagereng, 2011; Hashimoto and Kimura, 1999). The chert blocks in the mélange are deep marine deposits and show three distinct radiolarian assemblage ages from Late Jurassic to Late Cretaceous: late Tithonian, middle Valanginian to Barremian, and late Albian to Cenomanian (Jasin, 1996). The Lubok Antu Mélange formed in subduction-accretion setting and has been interpreted to be a lower Tertiary subduction complex which formed in an active subduction channel (Tan, 1982), or part of the Mesozoic accretion complex related to the subduction of

paleo-Pacific, assuming there is a continuous plate boundary from Southeast Asian to Borneo caused by the late Mesozoic subduction of the paleo-Pacific (Fig. 1B; Breitfeld et al., 2017; Hall and Breitfeld, 2017; Hennig et al., 2017).

Another mélange belt, the Boyan Mélange, is exposed to the south of the Lubok Antu Mélange (Fig. 1B, William et al., 1986, 1988). The relation of the Boyan Mélange and the Lubok Antu Mélange are uncertain. Metcalfe and Irving (1990) and Metcalfe (2011) considered that there is a small continental block, the Semitau block, sandwiched between the Lupar Line and the Boyan Mélange in West Sarawak, suggesting that these two mélange belts represent two separate accretionary belts. Williams et al. (1988) interpreted that the Boyan Mélange is a separate mélange belt to the south of the Lubok Antu Mélange, representing a former accretionary complex, as accretion proceeded, the locus of underthrusting migrated northward and the mélange ridge uplifted farther to the north. Breitfeld et al. (2017) considered that the Boyan Mélange is the southern continuation of the Lubok Antu Mélange, suggesting that there is a huge accretionary complex underlying most of the eastern part of the Kuching Zone and potentially the whole Sibu Zone (Fig. 1B).

The middle to late Eocene Silantek Formation is in faulted contact with or unconformably above the Lubok Antu Mélange in the north (Lupar Line 1 in Fig. 3B; Breitfeld et al., 2018; Galin et al., 2017; Tan, 1982). The Silantek Formation is composed of sandstone, mudstone, and basal conglomerate deposited in a floodplain and subsidiary fluvial environment (Breitfeld et al., 2018), and is intruded by early Miocene acid volcanics and stocks (Breitfeld et al., 2019).

To the north of the Lubok Antu Mélange, the Lupar Formation is assumed to be in a faulted contact with the Lubok Antu Mélange (Lupar Line 2 in Fig. 3B; Tan, 1982). The coherent Lupar Formation and Belaga Formation form the latest Cretaceous–Eocene northerly younging deep water turbiditic rocks of the Rajang Group (Fig. 4). The Lupar Formation is constituted by interbedded shale, mudstone, and sandstone, and is intruded by the Pakong Mafic Complex, a suit of gabbro, spilite, and basalt (Tan, 1982; Haile et al., 1994). The bedding-normal quartz veins in the Lupar Formation are mostly restricted to competent sandstone layers, suggesting large amount of fluid migration (Fig. 5F). The U-Pb age for youngest detrital zircon from the Lupar Formation suggest that the maximum depositional age (MDA) is 70 ± 1 Ma (Galin et al., 2017). The Belaga Formation is considered to be a deep water turbidite deposit consisting of Layar Member, Kapit Member, Pelagus Member, Metah Member, and Bawang Member from south to north (Fig. 4). Galin et al. (2017) divided the Belaga Formation into three units based on the heavy mineral assemblages and detrital zircons (Fig. 4). The sedimentological and petrographical characteristics of the Belaga Formation are very similar to the underlying Lupar Formation with MDA ages between 70 ± 1 Ma and 40 ± 1 Ma (Galin et al., 2017). The MDA is correlated well with the few published paleontological ages presented by Liechti et al. (1960) and Wolfenden (1960). The upper boundary of the Belaga Formation is well constrained at ca. 37 Ma based on the youngest zircons obtained from the Arip Volcanics (Hennig-Breitfeld et al., 2019). Tan (1982) and Honza et al. (2000) concluded that the turbidites of the Rajang Group are an accretionary prism based on the deep water and deformed character of the Rajang Group. Hutchison (2010) and Moss (1998) argued that subduction in Sarawak had ceased in the Late Cretaceous or Paleocene, and suggested that the older parts of the Rajang Group are an accretionary prism, but the younger turbidites of the Rajang Group were deposited in a remnant ocean basin. Breitfeld and Hall (2018) and Galin et al. (2017) considered that the Rajang Group was a turbidite fan in a passive setting and part of a large sediment system ranging from the Malay Peninsula through the present-day Sunda shelf. The basement of the Kuching Zone and the Sibu Zone has been considered by Breitfeld et al. (2017) to be the Cretaceous accretionary prism, during paleo-Pacific subduction, which formed the arc-related igneous rocks of the Schwaner Mountains. Thus, the Lubok Antu Mélange may be a part of the wide accretionary zone at the eastern margin of Asia (Breitfeld et al., 2017; Galin et al., 2017). The Rajang Group overlying the Lubok Antu Mélange is covered by upper Eocene conglomerate and finer grained shallow marine sediments, which indicates that there is a major unconformity (Rajang Unconformity; Hall and Breitfeld, 2017). The age of this major uplift phase was well constrained to 37–34 Ma in recent studies (Breitfeld et al., 2020b; Hennig-Breitfeld et al., 2019). The Rajang Unconformity is likely related to tectonic processes associated with the onset of subduction of the proto-South China Sea and/or the rotation of Borneo (Hall and Breitfeld, 2017; Hennig-Breitfeld et al., 2019).

APPLIED METHODOLOGIES

In order to reconstruct the time-constrained subduction process related to the formation of the Lubok Antu Mélange, pelitic matrix of the Lubok Antu Mélange and mudstone of the Lupar Formation were collected for vitrinite reflectance and illite age analysis.

Vitrinite Reflectance

We collected nine pelitic matrix and mudstone samples from the Lubok Antu Mélange and Lupar Formation for vitrinite reflectance analysis to explore the maximum paleotemperature during burial (Fig. 3A). The random reflectance (R_o) of vitrinite was measured on polished sections of concentrates of kerogen under a Carl Zeiss Axio Scope A1 Pol microscope equipped with a MSP 400 photometer. The extraction of the kerogen and the measurement of the vitrinite reflectance followed the National Standard of China GB/T 19144-2010 and SY/T 5124-2012, respectively. The maximum temperature was calculated by the mean random reflectance (R_m) based on the Barker (1988) method.

K-Ar Dating

We chose three samples (one from the mudstone of the coherent Lupar Formation, and two from the deformed pelitic matrix of the Lubok Antu Mélange; Figs. 3A and 3B) for K-Ar dating. The pelitic matrix which flows ductilely were chosen for dating. Thus, the illite K-Ar age may record deformation under conditions of unconsolidation or semi-consolidation (Figs. 5A and 5C). Petrographic investigations using optical microscopy indicate that our samples include detrital mica grains (Fig. 5H). The relative age contribution of the two K-bearing mineral phases (detrital/authigenic phase) can be better assessed by separating the sample into discrete grain sizes. To avoid artificial grain-size reduction, we first crushed samples by hand and removed small visible pieces of sandstone blocks in the mélange matrix, and then collected the remaining samples. Three grain size fractions (0.2–0.5, 0.5–1.0, and 1.0–2.0 μm) were separated by gravity settling using Stoke's law and high-speed centrifuging.

Mineralogical Observation

X-ray diffraction (XRD) patterns of oriented samples and random powder samples were used for clay identification and mineral quantification, respectively. Oriented samples prepared by drying 1 ml sample suspension on a glass slide were scanned over the ranges from 2° to 70° 2θ at the speed of 0.02° 2θ/s by the Rigaku MultiFlex diffractometer with diffracted-beam-monochromated CuKα radiation (36 kV, 16 mA) in Kochi University, Japan. The slides were also analyzed after one day glycolization. Random powder samples side-loaded into an Al sample

holder were scanned over angles of 2θ = 3–75° by the X'Pert Pro multi-purpose diffractometer with CuKα radiation (45 kV, 40 mA) at the Center for Advanced Marine Core Research, Kochi University, Japan.

Transmission electron microscopy (TEM) was used to investigate grain morphology and crystallography to verify the presence of illite in the fraction and evaluate the contamination of other K-bearing minerals. Detailed grain characterization of the grain size fraction (0.5–1.0 μm) of our samples was obtained using a JEOL JEM-ARM200F (200 kV) located at the Kochi Institute for Core Sample Research, Japan Agency for Marine-Earth Science and Technology. We first dispersed the fractions (0.5–1.0 μm) in ethanol and then added one or two drops of the supernatants onto the Cu grids and let them dry naturally in the air. High-resolution TEM imaging and selected-area electron diffraction (SAED) were used for identifying morphological and crystallographic structure, and the energy dispersive X-ray spectrometer attached to the TEM were used for investigating the chemical composition of individual grains.

K-Ar analysis

Isotopic dating analyses for selected fractions were undertaken in Hiruzen Institute for Geology and Chronology Co., Ltd., Japan. We used Teflon beakers containing a mixture of nitric acid and hydrofluoric acid to dissolve each fraction (~50 mg) for 12 h. The samples were then dried on a hot plate before being re-decomposed in HCl. The resulting solution was then used for potassium qualitative analysis by flame photometry. We ran each analysis twice, thus the reproducibility of our sample was confirmed. An average value was obtained for calculating the K-Ar age. Based on the multiple runs of two standards (JB-1 basalt and JG-1 granodiorite; Imai et al., 1995), the analytical error is within 2%. The analytical procedures are described in detail in Nagao et al. (1984).

For argon isotopic analysis, we first wrapped each fraction (~70–75 mg) in a thin aluminum foil and placed it in a sample holder and then used the ribbon and mantle heater to heat the sample for three days at 180–200 °C, thus the adsorption gas would release in a vacuum. Then we dropped the remaining sample into a molybdenum crucible and heated it to 1500 °C for half an hour, thus the activated gases (carbon, hydrogen, oxygen, and sulfur) were removed. Finally, we analyzed purified argon gas by using the mass spectrometer after the isotopic dilution method of Itaya et al. (1991). Multiple analyses of JG-1 biotite (ca. 91 Ma) were used as the standard (Itaya et al., 1991; Yagi et al., 2015), the standard deviation of the ^{38}Ar spike calibrations was determined to be within 1%. The analytical methods for calculating the age are described in detail in Nagao et al. (1984) and Nagao and Itaya (1988). The decay constants for ^{40}K to ^{40}Ar (0.581×10^{-10}/year), ^{40}Ca (4.962×10^{-10}/year), and ^{40}K content (1.167×10^{-4}) were used for the age calculation in potassium (Steiger and Jäger 1977). Ages with the 2σ confidence level were obtained.

Percentage of Detrital and Authigenic Illite

All fractions of each sample were measured by powder XRD. The authigenic ($1M/1M_d$ illite polytype)/detrital ($2M_1$ illite polytype) ratio was quantified using iterative full-pattern fitting by matching modeled XRD patterns generated by WILDFIRE and XRD patterns of our powder samples in the range of 20° to 37° 2θ (Reynolds, 1993; supporting information Fig. S1[1]). The goodness of fit by the full-pattern fitting method was determined by R% value ((Σ | (simulated-measured)/measured |) n * 100; Fisher et al., 2019; Song et al., 2014, Tonai et al., 2016). We estimate that the quantification error of the content of the detrital illite ($2M_1$ polytype) in the selected samples is within ± 5% according to the measurement error of duplicate samples. After assessing the proportion of authigenic and detrital illite in each fraction, three size fractions (0.2–0.5, 0.5–1.0, and 1.0–2.0 μm) of each sample were chosen for K-Ar dating.

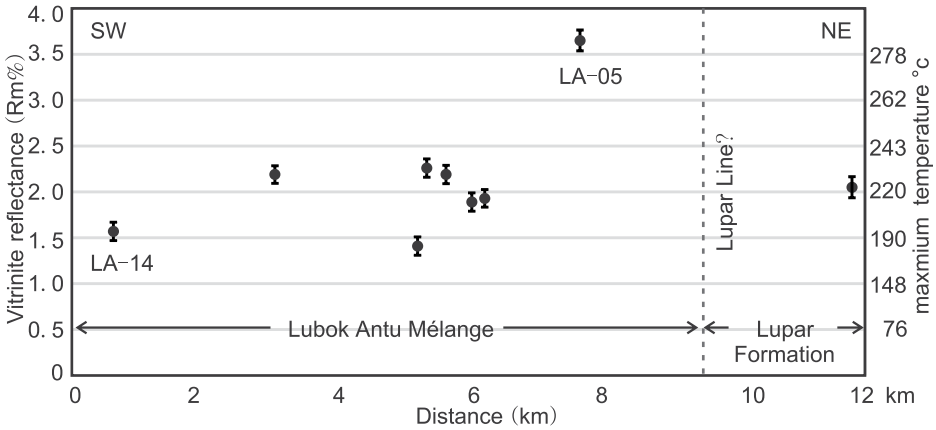

Figure 6. Paleothermal structure of the Lubok Antu Mélange and the coherent Lupar Formation, Sarawak, Borneo determined from vitrinite reflectance (R_m). The bars show the standard deviation (1σ).

RESULTS

Paleothermal Structure from Vitrinite Reflectance

R_m values have a high degree of confidence due to the standard deviation being less than 0.15 for each sample. The R_m values from the Lubok Antu Mélange are from 1.57% to 3.65% and the R_m value from the Lupar Formation is 2.05% (Fig. 6). The maximum paleotemperature of the K-Ar dating samples LA-14, LA-05, and LA-08, from south to north, were 195 ± 30 °C, 283 ± 30 °C, and 223 ± 30 °C, respectively (Fig. 6).

Mineralogical Characterization

X-ray semiquantitative analysis of various grain size fractions from the matrix of the Lubok Antu Mélange and the mudstone of the Lupar Formation are shown in Table 1. Mineral composition in each grain size fraction is almost the same, however, chlorite is not significant in LA-05, and coarser fractions contain more quartz (Table 1). The fractions contain few orthoclase grains. Detrital muscovite could be contained in these samples because its XRD pattern is identical to that of $2M_1$ polytype illite. Thus, K-Ar ages of the samples mainly reflect the contributions of authigenic illite and/or detrital muscovite.

TEM observations of the fractions (0.5–1.0 μm) show the typical crystal morphologies of illite (Freed and Peacor, 1992; Wilkinson et al., 2014), such as acicular and platy (Figs. 7A and 7B). SAED patterns show the reflection of these K and Al-rich illite particles is consistent with the 1.0 nm interlayer spacing of (001) of $1M/1M_d$ illite or (002) of $2M_1$ illite (Fig. 7C), while some of the illite grains show diffuse scattering of the non-001 reflections,

[1]Supplemental Material. Observed XRD patterns (black) and best matches (gray) generated by the program WILDFIRE for size fractions of our samples. Please visit https://doi.org/10.1130/GSAB.S.14356358 to access the supplemental material, and contact editing@geosociety.org with any questions.

TABLE 1. X-RAY SEMIQUANTITATIVE ANALYSIS OF VARIOUS GRAIN SIZE FRACTION FOR MATRIX OF THE LUBOK ANTU MÉLANGE AND MUDSTONE OF THE LUPAR FORMATION IN WEST SARAWAK, BORNEO

Grain size (μm)	Whole-rock composition (wt%)						
	Qtz	I/*M*-2M_1	I-1M_d	Chl	Kln	An	Ort
LA-14 Mélange (South)							
0.2–0.5	–	13	44	32	11	–	–
0.5–1.0	4	18	43	26	9	–	–
1.0–2.0	12	16	27	30	15	–	–
LA-05 Mélange (North)							
0.2–0.5	1	13	69	–	17	–	–
0.5–1.0	4	24	50	–	22	–	–
1.0–2.0	8	25	37	–	24	4	2
LA-08 Lupar Formation							
0.2–0.5	3	29	52	12	4	–	–
0.5–1.0	7	25	31	34	3	–	–
1.0–2.0	13	25	17	39	6	–	–

Note: An—anorthite; Chl—chlorite; I-1M_d—illite-11M_d; I/*M*-2M_1—illite/muscovite-2M_1; Kln—kaolinite; Ort—Orthoclase; Qtz—quartz.

suggesting the illite grains are 1M_d polytype (Fig. 7D; Grubb et al., 1991; Fisher et al., 2019). In general, the 2M_1 and 1M_d illite polytypes are abundant in this study, and there are no or very few other potassium-bearing minerals.

K-Ar Dating

The results of the K-Ar analysis of each fraction are shown in Table 2. The atmospheric argon contamination can be neglected and the analytical results are reliable, based on the non-radiogenic ^{40}Ar content (3.5%–4.4%). The potassium concentrations (3.2% to 4.8%) indicate that the analyzed samples are not high-purity illite, but also contain varying amounts of other potassium-free minerals, such as, the chlorite and quartz determined by the XRD patterns and TEM images.

For the mélange matrix samples, K-Ar dating results yielded ages between 81.5 ± 1.8 Ma and 93.7 ± 2.0 Ma for sample LA-14 and between 66.2 ± 1.5 Ma and 75.9 ± 1.7 Ma for sample LA-05. Sample LA-08 from the Lupar Formation yielded K-Ar ages of 45.9 ± 1.0 Ma, 48.3 ± 1.1 Ma, and 53.0 ± 1.2 Ma for the 0.2–0.5, 0.5–1.0, and 1.0–2.0 μm grain sizes, respectively (Table 2).

The modeling of observed XRD powder patterns for our samples indicates a systematic decrease in the value of the 2M_1/(2M_1+1M_d) illite polytype with decreasing grain size (Fig. S1; Table 2). The values of the 2M_1/(2M_1+1M_d) illite polytype are less than 40% in any size fraction from the samples of the mélange pelitic matrix (Fig. S1; Table 2). The modeling for the samples from the Lupar Formation indicates the values of the 2M_1 / (2M_1+1M_d) illite polytype are between 66.5% and 31.0% (Fig. S1; Table 2).

The results of IAA from three fractions of each mélange matrix and the Lupar Formation mudstone sample are shown in Figure 8. The plot shows a good linear relationship with the percentage of the 2M_1 illite polytype when the regression analysis is carried out (Fig. 8). The linear regression is based on the least-square linear regression with 1σ confidence intervals. The lower intercepts of the linear regressions, which correspond to the age of authigenic illite (1M_d polytype), are calculated as 62.2 ± 2.4 Ma for LA-14 (mélange matrix), 59.4 ± 4.1 Ma for LA-05 (mélange matrix), and 35.8 ± 0.1 Ma for LA-08 (Lupar Formation). The upper age intercepts, which correspond to the age of high-temperature illite or muscovite (2M_1 polytype), are calculated as 145 ± 5.1 Ma for LA-14 (mélange matrix), 96.2 ± 8.3 Ma for LA-05 (mélange matrix), and 63.7 ± 0.2 Ma for LA-08 (Lupar Formation).

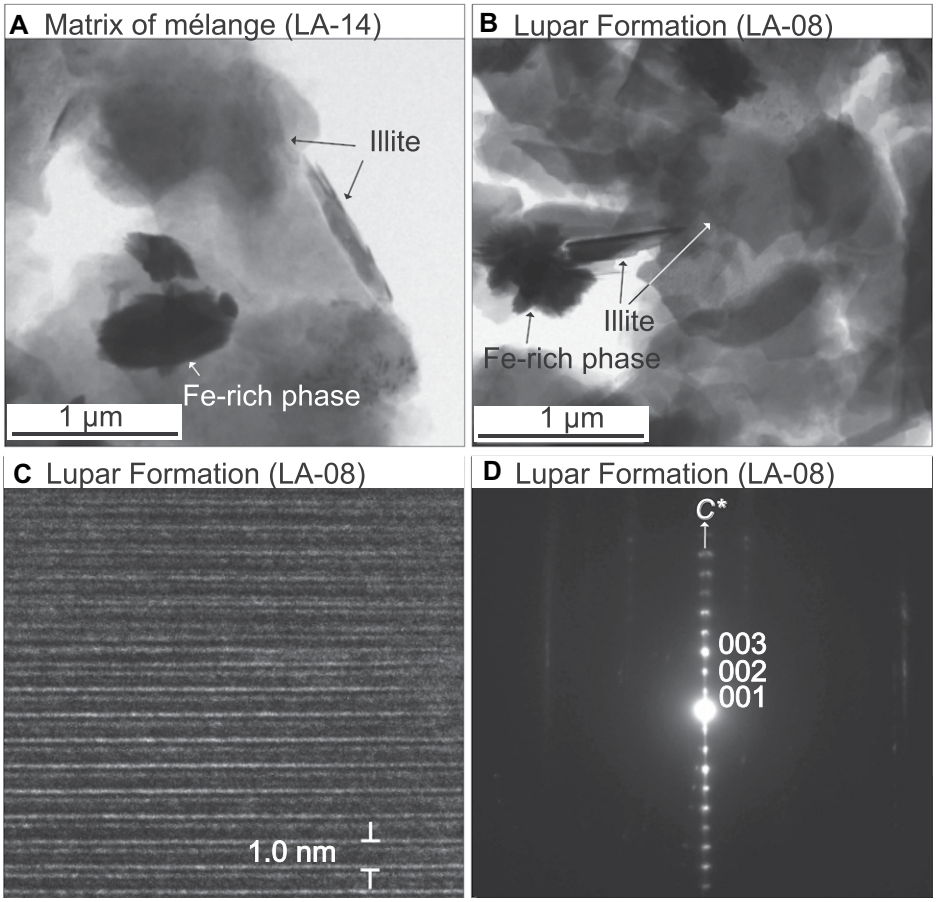

Figure 7. Transmission electron microscopy images (TEM) for the medium fractions samples (0.5–1.0 μm) in (A) the pelitic matrix shale of the Lubok Antu Mélange (LA-14) and (B) the mudstone of the Lupar Formation (LA-08), Sarawak, Borneo. (C) High-resolution TEM image and (D) electron diffraction pattern of an illite particle revealing a 1.0 nm interlayer spacing in the medium fractions of the Lupar Formation mudstone sample. Please attention that the diffuse scattering of the non-001 reflections suggests the acicular illite grain is 1M_d polytype (D).

DISCUSSION

The Meaning of Illite Polytypes

The estimates for the timing of illite authigenesis require an evaluation of whether the 2M_1 illite polytype in our samples is detrital. It has long been recognized that the mean particle size of authigenic illite in shale is generally finer than that of detrital illite/muscovite (Fisher et al., 2019; Pevear, 1992, 1999; Tonai et al., 2016). The XRD analyses show that the ratio of 2M_1

TABLE 2. K-Ar AGES AND THE $2M_1$ AMOUNT FOR ALL SIZE FRACTIONS OF THE LUBOK ANTU MATRIX AND THE LUPAR FORMATION MUDSTONE IN WEST SARAWAK, BORNEO

Grain size (μm)	K content (K_2O wt%)	Rad.^{40}Ar (10^{-8}cc^3 STP/g)	K-Ar age (Ma)	Non-rad.^{40}Ar (%)	$2M_1/(2M_1+1M_d)$ (%)
LA-14 Mélange (South)					
0.2–0.5	3.992 ± 0.080	1291.9 ± 13.1	81.5 ± 1.8	4.4	24.0 ± 5
0.5–1.0	3.716 ± 0.074	1301.5 ± 13.3	88.1 ± 1.9	4.1	30.0 ± 5
1.0–2.0	3.360 ± 0.067	1253.4 ± 12.8	93.7 ± 2.0	4.3	38.5 ± 5
LA-05 Mélange (North)					
0.2–0.5	4.780 ± 0.096	1250.5 ± 12.7	66.2 ± 1.5	4.1	16.5 ± 5
0.5–1.0	4.570 ± 0.091	1246.2 ± 12.6	68.9 ± 1.5	3.9	33.0 ± 5
1.0–2.0	3.991 ± 0.080	1200.7 ± 12.4	75.9 ± 1.7	3.5	40.0 ± 5
LA-08 Lupar Formation					
0.2–0.5	4.342 ± 0.087	782.6 ± 7.9	45.9 ± 1.0	3.7	36.0 ± 5
0.5–1.0	3.919 ± 0.078	744.1 ± 7.5	48.3 ± 1.1	3.6	45.0 ± 5
1.0–2.0	3.236 ± 0.065	675.0 ± 6.9	53.0 ± 1.2	4.3	61.5 ± 5

Note: The errors for obtained ages are at the 2σ confidence level. Rad.—Radiogenic; STP—Standard Temperature and Pressure: conditions of 0 °C and 1 atm.

illite polytype to $1M_d$ illite polytype components decreases with decreasing grain size in our samples, likely suggesting a mixture of detrital illite/muscovite ($2M_1$ illite polytype) and authigenic illite ($1M$/$1M_d$ illite polytype; Table 2).

For the Lubok Antu Mélange, the peak temperatures of LA-05 is identical within error to the crystallization temperature ~280 °C of $2M_1$ polytype (Srodon and Eberl, 1984), revealing that there may be some authigenic high-temperature or synkinematic $2M_1$ polytype. However, the latest depositional ages based on age-diagnostic fossils (Jasin, 1996) overlap with, or are broadly consistent with, the extrapolated age of the $2M_1$ polytype, indicating that the detrital illite/muscovite contributes a lot to the mélange matrix (Fig. 8). Thus, the $2M_1$ polytype from the pelitic matrix of the Lubok Antu Mélange may be mainly of detrital origin, as derived from the sedimentary history of the source area. Given that LA-14 and LA-05 show different 100% $2M_1$ polytype ages (145 ± 5.1 Ma for LA-14, 96.2 ± 8.3 Ma for LA-05), the $2M_1$ polytype illite/muscovite may be from different sources or a mixture with no geological significance (Song et al., 2014; van der Pluijm et al., 2006). However, the percentage of the $2M_1$ polytype component should be linearly related to age for the different clay size populations only if two distinct polytypes exist within the mixture. If a single clay sample contains detrital $2M_1$ polytype illite components with variable argon ages, then a linear relationship between illite percentage and age is highly unlikely because the $2M_1$ polytypes with variable ages are required to have the same relative proportions in all size fractions (Duvall et al., 2011). Our IAA plot shows a good linear relationship with the percentage of $2M_1$ illite polytype when the regression analysis is carried out (Fig. 8), and the $2M_1$ percentage correlates positively with grain size and total gas age (Table 2). Thus, different 100% $2M_1$ polytype ages in the mélange matrix samples might be a result of source changes, which awaits more regionally extensive data.

For the Lupar Formation, based on the youngest zircon U-Pb dates (72–70 Ma; Galin et al., 2017) and fossils (Turonian–Maastrichtian; Milroy, 1953), the $2M_1$ illite polytype may not be considered as a detrital contribution to the Lupar Formation as the depositional ages of the Lupar Formation are slightly older than the extrapolated age of the $2M_1$ illite polytype (63.7 ± 0.2 Ma; Fig. 8). An alternative interpretation is that the $2M_1$ polytype illite/muscovite in the Lupar Formation may represent the authigenic/synkinematic products of higher temperature fluid flow or regional deformation events (e.g., Aldega et al., 2019; Song et al., 2014; Torgersen et al., 2014).

TEM observations of the 0.5–1.0 μm fractions of the mélange matrix sample (LA-14) and the Lupar Formation sample (LA-08) reveal fine-grained illitic crystallites. The acicular and plate illite grains observed by the TEM and the $1M_d$ illite polytype shown by the SAED patterns indicate that these illite grains are authigenic (Fig. 7). Thus, the lower K-Ar age intercepts are interpreted to be the ages of the authigenic illite grains ($1M$/$1M_d$ illite polytype; Fig. 8).

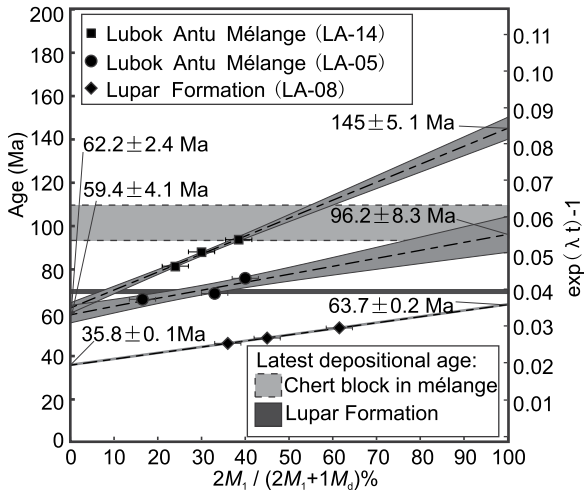

Figure 8. Illite age analysis plot of the value of $2M_1$ / ($2M_1$+$1M_d$) illite polytype and the K-Ar age for the Lubok Antu Mélange matrix samples and the Lupar Formation mudstone samples, Sarawak, Borneo. The function ($\exp_{(\lambda t)}$–1) has a linear correlation with the proportion of $2M_1$ illite polytype, where t is the measured radiometric time and λ is the total potassium decay constant. The dotted lines show linear regression. The shaded areas along the dotted lines represent confidence intervals (1σ) of the data.

Authigenic Illite Ages of the Mélange Pelitic Matrix: Paleocene Subduction

Orange and Underwood (1995) proposed that the thermal maturity can be used as diagnostic criteria for the classification of the mélange in ancient accretionary complexes. The R_m values of mélange formed along the subduction plate interface (2.15–3.45) is significantly higher than the R_m values of mélange formed under the conditions of gravitationally induced lateral spreading of the slope apron (0.4–0.5), large-scale mass wasting (olistostromes; 0.5–0.85), diapiric injection (1.35–1.85), and tectonic deformation within shear zones (0.75–1.75) (Orange and Underwood, 1995). Thus, R_m values from our samples are from 1.57% to 3.65%, with an average of 2.16%, suggesting the Lubok Antu Mélange formed along the subduction plate interface. The 184 °C to 283 °C paleotemperature estimates calculated from the R_m values also show that the mélange formed at seismogenic depth, which is typical for plate boundary tectonic mélanges (Kimura et al., 2012; Kitamura et al., 2005).

Non-coaxial extension and asymmetric fabrics of the sandstone blocks in the Lubok Antu Mélange indicate a top-to-north shearing, which is consistent with deformation along the plate interface during south-directed subduction (Figs. 5A–5D). Ductile matrix flow around asymmetric boudin suggests it deformed ductilely by dissolution-precipitation creep as the rocks lithified (Fig. 5E; e.g., Fagereng, 2011; Hashimoto and Kimura, 1999). Hand specimens also show the similar asymmetric fabrics (Fig. 5G). These fabrics indicate that the block-in-matrix structures of the Lubok Antu Mélange formed by shearing under conditions of unconsolidation or semi-consolidation and had gradually lithified during subduction (e.g., Hashimoto

and Kimura, 1999), suggesting the clay development was syntectonic (e.g., Zwingmann and Mancktelow, 2004). Thus, the paleotemperature, the general top-to-the-north shear sense, and the lithological composition with chert and turbidite components suggest that the Lubok Antu Mélange formed in a subduction-accretion setting is of tectonic origin caused by underthrusting and shearing along the subduction plate interface, and could be a chert-turbidite type ocean plate stratigraphy mélange (Festa et al., 2019; Wakita, 2015).

The deformation of the tectonic mélange formed along the subduction plate interface has been considered to be contemporaneous with burial and subduction, while other localized deformation structures were formed during a later stage than the mélange internal deformation based on the kinematics analysis and radiometric constraints (e.g., Bachmann et al., 2009; Raimbourg et al., 2019). Breitfeld et al. (2017, 2020a) reported that there was a potential shearing event in Sarawak and SW Borneo at ca. 25 Ma and interpreted it might be related to the Lupar Line trend and counter-clockwise rotation (Fuller et al., 1999; Schmidtke et al., 1990). Apatite fission-track ages in central Borneo also indicate a period of rapid denudation and uplift at that time (Moss et al., 1998). However, these late periods of shearing have not been recorded by our authigenic illite K-Ar ages of the Lubok Antu Mélange matrix. The synkinematic/authigenic illite age of the tectonic mélange matrix was not noticeably affected by later brittle deformation caused by the exhumation processes (e.g., the Mugi Mélange of the Shimanto accretionary complex, see Fisher et al., 2019; Tonai et al., 2016). Thus, the Lubok Antu Mélange could cease to serve as the locus of shear during the younger tectonic events, and the shear deformation was localized along shear zones such as the Lupar Line. Furthermore, our field observations also show that there is no penetrative overprint on the overall top-to-the-north sense of shear (Fig. 5), so that the primary textures of the tectonic mélange formed during the subduction-accretion process are preserved. The absence of the internal deformation style of the mélange in the nearby coherent unit (e.g., the Lupar Formation) also indicates that the mélange deformation was contemporaneous with subduction (e.g., Raimbourg et al., 2019).

The fault contact relationship (Lupar Line 2; Fig. 3A) between the Lubok Antu Mélange and the Lupar Formation is likely supported by a possible paleotemperature drop between them (Fig. 6). Thus, the Lupar Line may represent an out-of-sequence thrust that juxtaposed mélange-turbidite units (e.g., Ohmori et al., 1997), or an oblique strike-slip fault that exposed the Lubok Antu Mélange (Breitfeld et al., 2018; Breitfeld and Hall, 2018; Galin et al., 2017; Hall, 2012; Hall and Sevastjanova, 2012).

If the growth of authigenic illite below the closure temperature (T_c) of argon loss, the age of authigenic illite represents the time of formation, but not subsequent cooling when the sample passed through a particular thermal window or T_c (Duvall et al., 2011). According to the T_c equations of Dodson (1973) and muscovite diffusion parameters appropriate for a cylindrical geometry (activation energy E = 64 kcal/mol, frequency factor Do = 4 cm^2/s and effective diffusion radii ranging from 0.05 to 2 μm; Harrison et al., 2009) and cooling rates of 1–10 °C/Ma, the T_c of illite is estimated to be ~250–350 °C (Duvall et al., 2011). The maximum paleotemperature of LA-14 (mélange matrix, 195 ± 30 °C) is lower than the illite T_c, suggesting that the formation temperature of authigenic/synkinematic illite in LA-14 (mélange matrix) is also lower than the illite T_c. Thus, the age of authigenic/synkinematic illite of the mélange matrix (LA-14) should represent the time of formation in the process of syn-burial deformation.

The fabrics associated with shear deformation in clay-rich rocks are helpful to confirm the pretectonic or syn-tectonic origin of clay minerals (Fig. 5; Vrolijk et al., 2018; Zwingmann and Mancktelow, 2004; Zwingmann et al., 2004). Photomicrograph of the mélange matrix samples for K-Ar dating exhibit strongly preferred alignment of clay minerals (Fig. 5H). Thus, the K-Ar ages derived from authigenic/synkinematic illite separated from structurally well constrained pelitic matrix samples allow us to propose illite growth during shear deformation (Figs. 5A and 5C; e.g., Aldega et al., 2019; Tartaglia et al., 2020; Torgersen et al., 2014; Viola et al., 2016). In addition, previous studies (Mullin, 1961; Vrolijk et al., 2018) observed that acicular (fibrous) illite crystals are rarely found in shales, but are usually the result of rapid growth, such as shear deformation. Thus, the $1M_d$ illite polytype grains with acicular (fibrous) morphologies observed by TEM images (Fig. 7A) and XRD patterns suggest that abundant authigenic illite grains in the mélange matrix sample underwent a different dissolution-precipitation history, implying the dated authigenic illite were synkinematic.

Radiogenic ^{40}Ar loss could occur due to external heating after the formation of the authigenic illite. Incipient volume diffusion for grain sizes <0.2 μm may start at ~250 °C during heating-cooling pulses over 5 m.y. (Torgersen et al., 2014; Süssenberger et al., 2018). However, radiogenic ^{40}Ar loss can be disregarded below temperatures of ~350 °C during the rapid heating-cooling cycle of millennium size (Zwingmann et al., 2019). The maximum paleotemperature of LA-14 (mélange matrix; 195 ± 30 °C) are significantly lower than both, making Ar loss unlikely. Although, the maximum paleotemperature of LA-05 (mélange matrix) is over 250 °C, Ar diffusion may have taken place only if the documented temperatures were attained over a long-time frame. Given that LA-14 and LA-05 constrain the same 100% authigenic illite age (62.2 ± 2.4 Ma for LA-14, 59.4 ± 4.1 Ma for LA-05), it implies that peak temperatures of ~283 °C were relatively short-lived. Thus, the Lubok Antu Mélange could be immediately transferred to the upper levels of the accretionary complex as a result of subduction-accretion processes (e.g., Draut and Clift, 2013; Festa et al., 2019) and/or the subsequent strike-slip faulting along the Lupar Line (Hall, 2012; Breitfeld et al., 2017; Fig. 9). This is analogous to the Mesomélange Unit of the McHugh Complex in southern Alaska, which was interpreted as a subduction channel unit that was preserved above the newly accreting wedge of trench sediments (Clift et al., 2012). As the Lupar Formation was accreted it would have removed the mélange from the plate boundary, allowing its preservation (Fig. 9).

By combining these statistically identical ages with our structural observation, we conclude that the Lubok Antu Mélange could be transferred to the upper levels of the accretionary complex immediately after its formation/deformation along the plate boundary at ca. 60 Ma. The Lupar Line was active and facilitated the migration of mélange at that time (Fig. 9). The subsequent shearing events in Borneo were localized along shear zones such as the Lupar Line.

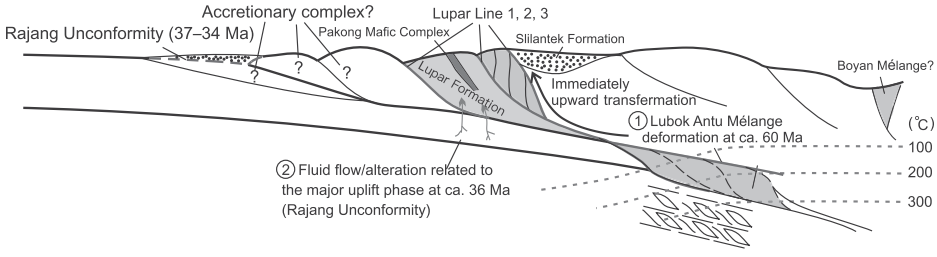

Figure 9. Cross section through Lupar Line based on K-Ar ages of the Lubok Antu Mélange matrix and Lupar Formation, showing the evolution of the Lubok Antu Mélange, Sarawak, Borneo.

Authigenic Illite Age of the Lupar Formation Mudstone: Rajang Unconformity

Our XRD results show that the Lupar Formation contains abundant $2M_1$ polytype illite/muscovite (31.5%–66.5%). The K-Ar age of the $2M_1$ polytype illite/muscovite (ca. 63 Ma) is slightly younger than the depositional age (Maastrichtian; Milroy, 1953; Galin et al., 2017) of the Lupar Formation, which indicate that the $2M_1$ polytype illite/muscovite in the Lupar Formation could crystallize authigenically/synkinematically during episode of fluid flow or regional deformation (e.g., Aldega et al., 2019; Song et al., 2014; Torgersen et al., 2014). There is no record of localized slip in the Lupar Formation, thus, the authigenesis of the $2M_1$ polytype illite/muscovite was more likely due to the hydrothermal fluids following igneous activity (e.g., Song et al., 2014; Viola et al., 2016).

Haile et al. (1994) concluded the basaltic lavas are interbedded with the Lupar Formation sediments, implying that the lavas were contemporaneous with the Lupar Formation. The intrusion of gabbro, of the same age or slight younger than the Lupar Formation, caused at least 50 m of contact metamorphism (Haile et al., 1994). Thus, the $2M_1$ illite/muscovite may be interpreted as products of the hydrothermal effect following these igneous activities (Pakong Mafic Complex).

Our extrapolated authigenic/synkinematic $1M_d$ illite age (35.8 ± 0.1 Ma) of the coherent Lupar Formation is obviously younger than the stratigraphic age. Under normal diagenetic conditions, the reaction process in clay minerals is irreversible, thus the uplifted stratum generally retain the chemical composition formed during maximum burial or maturity (Frey and Robinson, 1999). In addition, the timing of illite diagenesis is typically related to fluid flow/alteration in response to major tectonic events (e.g., Viola et al., 2016; Zhao et al., 1997). The possible diagenetic age, 35.8 ± 0.1 Ma, is almost the same as the Rajang Unconformity (37–34 Ma; Fig. 4; Breitfeld et al., 2020b; Hennig-Breitfeld et al., 2019), which implies that the $1M_d$ illite polytype component can be interpreted as the result of younger low-temperature fluid flow/alteration accompanying a major uplift phase at the timing of the Rajang Unconformity. The extensive distribution of bedding-normal quartz veins in the Lupar Formation further supports this statement (Fig. 5F).

Hutchison (2010) suggested that the beginning of shallow water carbonate deposition at the end of the Eocene both in central Sarawak and Kalimantan indicate the onset of the uplift phase, and described that the dramatic late Eocene change from deep water turbidites in the Sibu Zone to terrestrial/marginal marine sedimentary rocks within the Miri Zone was caused by the collision of the Luconia block following closure of the proto-South China Sea at ca. 37 Ma. However, Hall (2013), Hall and Breitfeld (2017), and Hall and Sevastjanova (2012) questioned the collision interpretation, and considered that the subduction of oceanic crust beneath Sarawak ceased at ca. 85 Ma and was completed long before subduction of the proto-South China Sea beneath Sabah and Cagayan began in the Eocene. Thus, the ocean crust subducted beneath Sarawak was most likely to be the paleo-Pacific. Hall and Breitfeld (2017) and Hennig-Breitfeld et al. (2019) attribute the Rajang Unconformity to the onset of subduction of the proto-South China Sea beneath Sabah and Cagayan and/or to the rotation of Borneo.

We have concluded above that the tectonic mélange ceased to serve as the locus of significant deformation after its formation, and the subsequent shearing events were localized along shear zones such as the Lupar Line. However, the matrix of the Lubok Antu Mélange also does not yield K-Ar ages related to the fluid flow/alteration in response to the major uplift phase (the Rajang Unconformity). As suggested above, the Lubok Antu Mélange was immediately transferred to the upper levels of the subduction accretion complex after its formation. Thus, the Lubok Antu Mélange was under shallower and/or cooler pressure-temperature conditions than the Lupar Formation, suggesting the absence of the fluid flow/alteration favorable to illite authigenic growth during this major uplift phase (e.g., Aldega et al., 2019; Fig. 9).

Implications for Paleogene Tectonic Evolution of Borneo

The first illite K-Ar ages obtained in this study provide new constraints on the tectonic evolution of Borneo. The ages of authigenic/synkinematic illite and the maximum paleotemperatures of dated samples indicate that the Lubok Antu Mélange could be uplifted immediately after its formation/deformation along the plate boundary at ca. 60 Ma. This interpretation is consistent with Hutchison (2005, 2010) who argued that the subduction in Sarawak could have continued until the Paleocene before most of the deep marine Rajang Group was deposited in a remnant ocean basin.

However, based on ages and geochemistry similarities, Hennig et al. (2017) suggested that the Cretaceous subduction-related rocks in the Schwaner Mountains formed during subduction at the paleo-Pacific margin after SW Borneo arrived at the Sundaland margin at ca. 135 Ma. Subduction-related magmatism in SW Borneo had ceased after collision of the Argo block (East Java-West Sulawesi) with SW Borneo at ca. 90 Ma at the Meratus Suture (Fig. 1B; Hall et al., 2009; Hall, 2012) and was then followed by the K-rich A-/S-/I-type granitoids of ca. 78–85 Ma and the A-type 72 Ma granites in the southern Schwaner Mountains (Breitfeld et al., 2020a; Davies et al., 2014). The age of the Pedawan Unconformity in the Kuching Zone also coincides with the termination of subduction-related magmatism in SW Borneo (Fig. 4; Breitfeld et al., 2018). Thus, several studies suggested that subduction beneath Sarawak also ceased at ca. 90 Ma (Breitfeld et al., 2017; Hennig et al., 2017; Breitfeld et al., 2020a). But it is noteworthy that Davies et al. (2014) and Hall (2012) argued that the subduction-related granites in SW Borneo are not the result of the Asian margin magmatism but are the result of south-directed subduction beneath SW Borneo during northward drifting of the SW Borneo block and widening of the Ceno-Tethys. Thus, the volcanic arc corresponding to subduction beneath Sarawak is unclear. However, samples from the Pueh and Gading intrusions in West Sarawak with ages ranging from 77 to 80 Ma, respectively, (mean ages of ca. 81 Ma) have chemical compositions of volcanic arc granite, their post-collisional character is thus uncertain. An alternative interpretation is that subduction-related magmatism in West Sarawak did not finish until ca. 81 Ma (Hennig et al., 2017).

Breitfeld and Hall (2018) and Galin et al. (2017) reported that a small number of Paleogene zircons in the Cenozoic sediments of Sarawak were likely derived from contemporaneous magmatism in Borneo, and interpreted that the very localized magmatism in Borneo does not support prolonged arc magmatism related to subduction in the Paleogene. However, arc magmatism resulting from subduction is not necessarily active throughout the history of an active margin (e.g., Macpherson and Hall, 2002; Yang et al., 2020). For example, the magmatic arc gap during the subduction of the Neo-Tethys ocean in the southern Tibet regions from ca. 145 to 120 Ma (Xiong et al., 2016), and the magmatic arc gap during the subduction of the Piemonte-Ligurian ocean in the Alps regions from ca. 100 to 50 Ma (McCarthy et al., 2018). Many causes, such as, flat-slab subduction (Hao et al., 2019; Kapp et al., 2005), slab breakoff (Butler and Beaumont, 2017), forearc hyperextension and/or trench migration (Maffione et al., 2015; Xiong et al., 2016), and mantle serpentinization and ocean crust delamination (Yang et al., 2020), may be responsible for the arc gap. In addition, several active subduction zones around our study region, such as, the North Sulawesi Trench, the

Philippine Trench, and Northern Borneo also have no or little subduction-related magmatism (Hall, 2009; Hall and Breitfeld, 2017). The Paleocene gap in arc magmatism in Borneo could be caused by flat-slab subduction at a very low speed (e.g., Williams et al., 1988). Or the ca. 60 Ma age can instead be interpreted as representing the final stage of subduction under Sarawak based on the absence/rarity of arc magmatism and the rapid uplift of the Lubok Antu Mélange after its formation/deformation at ca. 60 Ma.

Morley (1998) and Breitfeld et al. (2018) identified an abrupt shift in sedimentation within the Kayan Formation from deltaic to alluvial fan deposits (named Bungo Unconformity; Fig. 4) at ca. 56 Ma. Considering the paleocurrent observations of Tan (1984) and Breitfeld et al. (2018), Breitfeld and Hall (2018) suggested that the fresh input heavy mineral (garnet, epidote, apatite, titanite) into the upper Kayan Formation (named Penrissen Sandstone) indicates some sort of uplift in the eastern part of West Sarawak. An earlier ~40° counter-clockwise rotation of Borneo sometime between deposition of the Pedawan Formation (ca. 80 Ma) and the Tutoop/Silantek Formation (ca. 40 Ma) discussed by Schmidtke et al. (1990) and Fuller et al. (1999) might be associated with this uplift phase. Thus, the Lupar Line might have transferred into strike-slip faults at that time, which facilitated the migration of the mélange and was responsible for the development of the pull-apart basin (the Ketungau Basin) south of the Lupar Line (Hall, 2012; Breitfeld and Hall, 2018).

The subduction under Sarawak is not directly related to the opening of the South China Sea, thus it is confusing to name it proto-South China Sea (Hall and Breitfeld, 2017). Hall and Breitfeld. (2017) suggest that the term proto-South China Sea should be used only for the slab subducted beneath Sabah and Cagayan between the Eocene and early Miocene. Oceanic crust subducted during earlier episodes under Borneo should be termed paleo-Pacific. The three distinct radiolarian assemblage ages of chert blocks in the Lubok Antu Mélange ranges from Late Jurassic to Late Cretaceous, suggesting that the older oceanic basin is more like the paleo–Pacific Plate (Jasin, 1996). In addition, the very thick Rajang Group suggest that there is a huge amount of sediments supply, which is quite different from the open ocean. Thus, we suggest that the Lubok Antu Mélange represent a tectonic mélange related to the final stage of subduction of the embayment of the paleo-Pacific in Sarawak.

The ca. 36 Ma age matches well with the timing of the Rajang Unconformity (Breitfeld et al., 2020b; Hennig-Breitfeld et al., 2019). Hutchison (1996) interpreted it as the result of the Luconia block colliding with SW Borneo (Sarawak Orogeny), implying that the subduction in Sarawak continued until the late Eocene and the entire Rajang Group represents an accretionary complex. It is possible because the huge amount of sediments supplied to the embayment of the paleo-Pacific may obscure the architecture of the accretionary complex. However, our study suggests that the formation/deformation of the Lubok Antu Mélange could represent the final stage of subduction beneath Sarawak. Thus, an alternative interpretation is that the onset of subduction of the proto-South China Sea beneath Sabah and Cagayan and/or the rotation of Borneo led to the major uplift phase at ca. 37 Ma (Hall and Breitfeld, 2017; Hennig-Breitfeld et al., 2019).

CONCLUSIONS

Our study offers a new illite K-Ar dating application to constrain the age of deformation of the matrix in tectonic mélange formed in subduction-accretion setting. The ca. 60 Ma ages of authigenic illite combined with the paleotemperature data indicate that the Lubok Antu Mélange formed along the subduction plate boundary during the final stage of the subduction-accretion process. The ca. 36 Ma age of authigenic illite is almost the same as the Rajang Unconformity, representing the major uplift phase in West Sarawak. In addition to regional considerations, the proposed approach demonstrates that illite age analysis can be used successfully to date the timing of subduction when the fabric of mélanges records deformation during subduction-accretion process. Though earlier formed tectonic mélange have sometimes been influenced by later deformation, deconvoluting protracted brittle deformation can be performed by the K-Ar age analysis of authigenic illite (Viola et al., 2016). Thus, we consider that this method can be used to determine the timing of subduction, tectonic accretion, and exhumation histories by dating the tectonic mélange and associated faults formed in an accretionary complex if a comprehensive structural analysis is conducted.

ACKNOWLEDGMENTS

The National Natural Science Foundation of China (grant U1701641), the Key Special Project for Introduced Talents Team of Southern Marine Science and Engineering Guangdong Laboratory (Guangzhou) (grant GML 2019ZD0205), and the Innovation Academy of South China Sea Ecology and Environmental Engineering (grant ISEE2020YB07) and the Frontier Research Team of Marine Science of CAS Center for Excellence in Deep Earth Science are gratefully thanked for their financial support. Clift thanks the Charles T. McCord Jr. Chair in Petroleum Geology at Louisiana State University. We thank the Science Editor (Brad Singer), Associate Editor (William Guenthner), and reviewers (H. Tim Breitfeld, Espen Torgersen, and Robert Hall) for their constructive comments.

REFERENCES CITED

Aldega, L., Viola, G., Casas-Sainz, A., Marcén, M., Román-Berdiel, T., and van der Lelij, R., 2019, Unravelling multiple thermo-tectonic events accommodated by crustal-scale faults in northern Iberia, Spain: Insights from K-Ar dating of clay gouges: Tectonics, v. 38, no. 10, p. 3629–3651, https://doi.org/10.1029/2019TC005585.

Bachmann, R., Oncken, O., Glodny, J., Seifert, W., Georgieva, V., and Sudo, M., 2009, Exposed plate interface in the European Alps reveals fabric styles and gradients related to an ancient seismogenic coupling zone: Journal of Geophysical Research. Solid Earth, v. 114, no. B5, https://doi.org/10.1029/2008JB005927.

Barker, C.E., 1988, Geothermics of petroleum systems: Implications of the stabilization of kerogen thermal maturation after a geologically brief heating duration at peak temperature, *in* Magoon, L., ed., Petroleum Systems of the United States: U.S. Geological Survey Bulletin 1870, p. 26–29.

Breitfeld, H.T., and Hall, R., 2018, The eastern Sundaland margin in the latest Cretaceous to Late Eocene: Sediment provenance and depositional setting of the Kuching and Sibu Zones of Borneo: Gondwana Research, v. 63, p. 34–64, https://doi.org/10.1016/j.gr.2018.06.001.

Breitfeld, H.T., Hall, R., Galin, T., Forster, M.A., and Bou-Dagher-Fadel, M.K., 2017, A Triassic to Cretaceous Sundaland–Pacific subduction margin in West Sarawak, Borneo: Tectonophysics, v. 694, p. 35–56, https://doi.org/10.1016/j.tecto.2016.11.034.

Breitfeld, H.T., Hall, R., Galin, T., and BouDagher-Fadel, M.K., 2018, Unravelling the stratigraphy and sedimentation history of the uppermost Cretaceous to Eocene sediments of the Kuching Zone in West Sarawak (Malaysia), Borneo: Journal of Southeast Asian Earth Sciences, v. 160, p. 200–223, https://doi.org/10.1016/j.jseaes.2018.04.029.

Breitfeld, H.T., Macpherson, C., Hall, R., Thirlwall, M., Ottley, C.J., and Hennig-Breitfeld, J., 2019, Adakites without a slab: Remelting of hydrous basalt in the crust and shallow mantle of Borneo to produce the Miocene Sintang Suite and Bau Suite magmatism of West Sarawak: Lithos, v. 344–345, p. 100–121, https://doi.org/10.1016/j.lithos.2019.06.016.

Breitfeld, H.T., Davies, L., Hall, R., Armstrong, R., Forster, M., Lister, G., Thirlwall, M., Grassineau, N., Hennig-Breitfeld, J., and van Hattum, M.W.A., 2020a, Mesozoic Paleo- Pacific Subduction Beneath SW Borneo: U-Pb Geochronology of the Schwaner Granitoids and the Pinoh Metamorphic Group: Frontiers of Earth Science, v. 8, no. 568715, https://doi.org/10.3389/feart.2020.568715.

Breitfeld, H.T., Hennig-Breitfeld, J., BouDagher-Fadel, M.K., Hall, R., and Galin, T., 2020b, Oligocene-Miocene drainage evolution of NW Borneo: Stratigraphy, sedimentology and provenance of Tatau-Nyalau province sediments: Journal of Asian Earth Sciences, v. 195, no. 104331, https://doi.org/10.1016/j.jseaes.2020.104331.

Butler, J.P., and Beaumont, C., 2017, Subduction zone decoupling/retreat modeling explains South Tibet (Xigaze) and other supra-subduction zone ophiolites and their UHP mineral phases: Earth and Planetary Science Letters, v. 463, p. 101–117, https://doi.org/10.1016/j.epsl.2017.01.025.

Carboni, F., Viola, G., Aldega, G., van der Lelij, R., Brozzetti, F., and Barchi, M.R., 2020, K-Ar fault gouge dating of Neogene thrusting: The case of the siliciclastic deposits of the Trasomeno Tectonic Wedge (Northern Apennines, Italy): Italian Journal of Geosciences, v. 139, p. 300–308, https://doi.org/10.3301/IJG.2020.06.

Clauer, N., Srodon, J., Francu, J., and Sucha, V., 1997, K-Ar dating of illite fundamental particles separated from illite-smectite: Clay Minerals, v. 32, p. 181–196, https://doi.org/10.1180/claymin.1997.032.2.02.

Clauer, N., Zwingmann, H., Liewig, N., and Wendling, R., 2012, Comparative $^{40}Ar/^{39}Ar$ and K-Ar dating of illite-type clay minerals: A tentative explanation for the age identities and differences: Earth-Science Reviews, v. 115, p. 76–96, https://doi.org/10.1016/j.earscirev.2012.07.003.

Clift, P.D., Wares, N.M., Amato, J.M., Pavlis, T.L., Hole, M.J., Worthman, C., and Day, E., 2012, Evolving heavy

mineral assemblages reveal changing exhumation and trench tectonics in the Mesozoic Chugach accretionary complex, South-Central Alaska: Geological Society of America Bulletin, v. 124, no. 5-6, p. 989–1006, https://doi.org/10.1130/B30594.1.

Davies, L., Hall, R., and Armstrong, R., 2014, Cretaceous crust in SW Borneo: Petrological, geochemical and geochronological constraints from the Schwaner Mountains, *in* Proceedings Indonesian Petroleum Association, 38th Annual Convention, IPA14-G-025, Jakarta, Indonesia, 21–23 May, https://doi.org/10.29118/ipa.0.14.g.025.

Dodson, M.H., 1973, Closure temperature in cooling geochronological and petrological systems: Contributions to Mineralogy and Petrology, v. 40, p. 259–274, https://doi.org/10.1007/BF00373790.

Domeier, M., Magni, V., Hounslow, M.W., and Torsvik, T.H., 2018, Episodic zircon age spectra mimic fluctuations in subduction: Scientific Reports, v. 8, p. 17471, https://doi.org/10.1038/s41598-018-35040-z.

Doutch, H.F., 1992, Aspects of the structural histories of the Tertiary sedimentary basins of East, Central and West Kalimantan and their margins: BMR Journal of Australian Geology and Geophysics, v. 13, p. 237–250.

Draut, A.E., and Clift, P.D., 2013, Differential preservation in the geologic record of intraoceanic arc sedimentary and tectonic processes: Earth-Science Reviews, v. 116, p. 57–84, https://doi.org/10.1016/j.earscirev.2012.11.003.

Duvall, A.R., Clark, M.K., van der Pluijm, B.A., and Li, C., 2011, Direct dating of Eocene reverse faulting in northeastern Tibet using Ar-dating of fault clays and low-temperature thermochronometry: Earth and Planetary Science Letters, v. 304, p. 520–526, https://doi.org/10.1016/j.epsl.2011.02.028.

Fagereng, Å., 2011, Geology of the seismogenic subduction thrust interface, *in* Fagereng, Å., Toy, V.G., and Rowland, J.V., eds., Geology of the Earthquake Source: A Volume in Honour of Rick Sibson: Geological Society of London, Special Publication 359, p. 55–76, https://doi.org/10.1144/SP359.4.

Fagereng, Å., and Den Hartog, S.A.M., 2017, Subduction megathrust creep governed by pressure solution and frictional-viscous flow: Nature Geoscience, v. 10, p. 51–57, https://doi.org/10.1038/ngeo2857.

Fagereng, Å., and Sibson, R.H., 2010, Mélange rheology and seismic style: Geology, v. 38, p. 751–754, https://doi.org/10.1130/G30868.1.

Festa, A., Pini, G.A., Dilek, Y., and Codegone, G., 2010, Mélanges and mélange-forming processes: A historical overview and new concepts, *in* Dilek, Y., ed., Alpine Concept in Geology: International Geology Review, v. 52, p. 1040–1105. https://doi.org/10.1080/00206810903557704.

Festa, A., Dilek, Y., Pini, G.A., Codegone, G., and Ogata, K., 2012, Mechanisms and processes of stratal disruption and mixing in the development of mélanges and broken formations: Redefining and classifying mélanges: Tectonophysics, v. 568–569, p. 7–24, https://doi.org/10.1016/j.tecto.2012.05.021.

Festa, A., Pini, G.A., Ogata, K., and Dilek, Y., 2019, Diagnostic features and field-criteria in recognition of tectonic, sedimentary and diapiric mélanges in orogenic belt and exhumed subduction-accretion complexes: Gondwana Research, v. 74, p. 7–30, https://doi.org/10.1016/j.gr.2019.01.003.

Fisher, D.M., Tonai, S., Hashimoto, Y., Tomioka, N., and Oakley, D., 2019, K-Ar dating of fossil seismogenic thrusts in the Shimanto accretionary complex, southwest Japan: Tectonics, v. 38, no. 11, https://doi.org/10.1029/2019TC005571.

Freed, R.L., and Peacor, D.R., 1992, Diagenesis and the formation of authigenic illite-rich crystals in Gulf Coast shales: TEM study of clay separates: Journal of Sedimentary Petrology, v. 62, p. 220–234, https://doi.org/10.1306/D42678CA-2B26-11D7-8648000102C1865D.

Frey, M., and Robinson, D., 1999, Low-Grade Metamorphism: Oxford, UK, Blackwell Science Ltd., 313 p., https://doi.org/10.1002/9781444313345.

Fuller, M., Ali, J.R., Moss, S.J., Frost, G.M., Richter, B., and Mahfi, A., 1999, Paleomagnetism of Borneo: Journal of Asian Earth Sciences, v. 17, p. 3–24, https://doi.org/10.1016/S0743-9547(98)00057-9.

Galin, T., Tim Breitfeld, H., Hall, R., and Sevastjanova, I., 2017, Provenance of the Cretaceous–Eocene Rajang Group submarine fan, Sarawak, Malaysia from light and heavy mineral analysis and U-Pb Zircon geochronology: Gondwana Research, v. 51, p. 209–233, https://doi.org/10.1016/j.gr.2017.07.016.

Grathoff, G., Moore, D., Hay, R., and Wemmer, K., 1998, Illite polytype quantification in Paleozoic shales: A technique to quantify diagenetic and detrital illite, *in* Schieber, J., et al., eds., Shale and Mudstones II. Petrography, Petrophysics, Geochemistry, and Economic Geology: Stuttgart, Germany, Schweizerbartsche Verlagsbuchhandlung, p. 161–175.

Grathoff, G., Moore, D., Hay, R., and Wemmer, K., 2001, Origin of illite in the lower Paleozoic of the Illinois Basin: Evidence for brine migration: Geological Society of America Bulletin, v. 113, p. 1092–1104, https://doi.org/10.1130/0016-7606(2001)113<1092:OOIITL>2.0.CO;2.

Grubb, S.M.B., Peacor, D.R., and Jiang, W.T., 1991, Transmission electron microscope observations of illite polytypism: Clays and Clay Minerals, v. 39, p. 540–550, https://doi.org/10.1346/CCMN.1991.0390509.

Haile, N.S., 1974, Borneo, *in* Spencer, A.M., ed., Mesozoic-Cenozoic Orogenic Belts: Geological Society of London, Special Publication 4, p. 333–347.

Haile, N.S., Lam, S.K., and Banda, R.M., 1994, Relationship of gabbro and pillow lavas in the Lupar Formation, West Sarawak: Implications for interpretation of the Lubok Antu Melange and the Lupar Line: Bulletin of the Geological Society of Malaysia, v. 36, p. 1–9, https://doi.org/10.7186/bgsm36199401.

Haines, S.H., and van der Pluijm, B.A., 2008, Clay quantification and Ar-Ar dating of synthetic and natural gouge: Application to the Miocene Sierra Mazatán detachment fault, Sonora, Mexico: Journal of Structural Geology, v. 30, p. 525–538, https://doi.org/10.1016/j.jsg.2007.11.012.

Hall, R., 2009, Hydrocarbon basins in SE Asia: Understanding why they are there: Petroleum Geoscience, v. 15, p. 131–146, https://doi.org/10.1144/1354-079309-830.

Hall, R., Clements, B., and Smyth, H.R., 2009, Sundaland: Basement character, structure and plate tectonic development, *in* Proceedings Indonesian Petroleum Association, 33rd Annual Convention, IPA09-G-134, Jakarta, Indonesia, 5-7 May, p. 1–27.

Hall, R., 2012, Late Jurassic–Cenozoic reconstructions of the Indonesian region and the Indian Ocean: Tectonophysics, v. 570–571, p. 1–41, https://doi.org/10.1016/j.tecto.2012.04.021.

Hall, R., 2013, Contraction and extension in northern Borneo driven by subduction rollback: Journal of Asian Earth Sciences, v. 76, p. 399–411, https://doi.org/10.1016/j.jseaes.2013.04.010.

Hall, R., and Breitfeld, T., 2017, Nature and demise of the Proto-South China Sea: Bulletin of the Geological Society of Malaysia, v. 63, p. 61–76, https://doi.org/10.7186/bgsm63201703.

Hall, R., and Sevastjanova, I., 2012, Australian crust in Indonesia: Australian Journal of Earth Sciences, v. 59, p. 827–844, https://doi.org/10.1080/08120099.2012.692335.

Hao, L.-L., Wang, Q., Zhang, C., Ou, Q., Yang, J.-H., Dan, W., and Jiang, Z.-Q., 2019, Oceanic plateau subduction during closure of the Bangong-Nujiang Tethyan Ocean: Insights from central Tibetan volcanic rocks: Geological Society of America Bulletin, v. 131, p. 864–880, https://doi.org/10.1130/B32045.1.

Harrison, T.M., Célérier, J., Aikman, A.B., Hermann, J., and Heizler, M.T., 2009, Diffusion of ^{40}Ar in muscovite: Geochimica et Cosmochimica Acta, v. 73, no. 4, p. 1039–1051, https://doi.org/10.1016/j.gca.2008.09.038.

Hashimoto, Y., and Kimura, G., 1999, Underplating process from mélange formation to duplexing: Example from the Cretaceous Shimanto Belt, Kii Peninsula, southwest Japan: Tectonics, v. 18, p. 92–107, https://doi.org/10.1029/1998TC900014.

Hennig, J., Breitfeld, H.T., Hall, R., and Nugraha, A.M.S., 2017, The Mesozoic tectono-magmatic evolution at the Paleo-Pacific subduction zone in West Borneo: Gondwana Research, v. 48, p. 292–310, https://doi.org/10.1016/j.gr.2017.05.001.

Hennig-Breitfeld, J., Breitfeld, H.T., Hall, R., BouDagher-Fadel, M., and Thirlwall, M., 2019, A new upper Paleogene to Neogene stratigraphy for Sarawak and Labuan in north-western Borneo: Paleogeography of the eastern Sundaland margin: Earth-Science Reviews, v. 190, p. 1–32, https://doi.org/10.1016/j.earscirev.2018.12.006.

Honza, E., John, J., and Banda, R.M., 2000, An imbrication model for the Rajang accretionary complex in Sarawak, Borneo: Journal of Asian Earth Sciences, v. 18, p. 751–759, https://doi.org/10.1016/S1367-9120(00)00044-4.

Hower, J., Hurley, P.M., Pinson, W.H., and Fairbairn, H.W., 1963, The dependence of K-Ar age on the mineralogy of various particle size ranges in a shale: Geochimica et Cosmochimica Acta, v. 27, p. 405–410, https://doi.org/10.1016/0016-7037(63)90080-2.

Hutchison, C.S., 1996, The 'Rajang accretionary prism' and 'Lupar Line' problem of Borneo, *in* Hall, R., and Blundell, D., eds., Tectonic Evolution of Southeast Asia: Geological Society of London, Special Publications 106, p. 247–261, https://doi.org/10.1144/GSL.SP.1996.106.01.16.

Hutchison, C.S., 2005, Geology of North-West Borneo: Sarawak, Brunei and Sabah: Amsterdam, The Netherlands, Elsevier, 421 p.

Hutchison, C.S., 2010, Oroclines and paleomagnetism in Borneo and South-East Asia: Tectonophysics, v. 496, p. 53–67, https://doi.org/10.1016/j.tecto.2010.10.008.

Imai, N., Terashima, S., Itoh, S., and Ando, A., 1995, 1994 compilation values for GSJ reference samples, "Igneous rock series": Geochemical Journal, v. 29, p. 91–95, https://doi.org/10.2343/geochemj.29.91.

Itaya, T., Nagao, K., Inoue, K., Honjou, Y., Okada, T., and Ogata, A., 1991, Argon isotope analysis by a newly developed mass spectrometric system for K-Ar dating: Mineralogical Journal, v. 15, p. 203–221, https://doi.org/10.2465/minerj.15.203.

Jasin, B., 1996, Late Jurassic to Early Cretaceous Radiolaria from chert blocks in the Lubok Antu mélange, Sarawak, Malaysia: Journal of Southeast Asian Earth Sciences, v. 13, p. 1–11, https://doi.org/10.1016/0743-9547(96)00001-3.

Kapp, P., Yin, A., Harrison, T.M., and Ding, L., 2005, Cretaceous-Tertiary shortening, basin development, and volcanism in central Tibet: Geological Society of America Bulletin, v. 117, p. 865–878, https://doi.org/10.1130/B25595.1.

Kimura, G., Yamaguchi, A., Hojo, M., Kitamura, Y., Kameda, J., Ujiie, K., Hamada, Y., Hamahashi, M., and Hina, S., 2012, Tectonic mélange as fault rock of subduction plate boundary: Tectonophysics, v. 568–569, p. 25–38, https://doi.org/10.1016/j.tecto.2011.08.025.

Kitamura, Y., Sato, K., Ikesawa, E., Ikehara-Ohmori, K., Kimura, G., Kondo, H., Ujiie, K., Onishi, C.T., Kawabata, K., Hashimoto, Y., Mukoyoshi, H., and Masago, H., 2005, Mélange and its seismogenic roof décollement: A plate boundary fault rock in the subduction zone: An example from the Shimanto Belt, Japan: Tectonics, v. 24, no. 5, https://doi.org/10.1029/2004TC001635.

Kula, J., Spell, T.L., and Zanetti, K.A., 2010, Ar/Ar analyses of artificially mixed micas and the treatment of complex age spectra from samples with multiple mica populations: Chemical Geology, v. 275, p. 67–77, https://doi.org/10.1016/j.chemgeo.2010.04.015.

Kunk, M.J., and Brusewitz, A.M., 1987, ^{39}Ar recoil in an I/S clay from the Ordovician "Big Bentonite Bed" at Kinnekulle, Sweden: Geological Society of America Abstracts with Programs, v. 19, p. 230.

Liechti, P., Roe, F.W., and Haile, N.S., 1960, The geology of Sarawak, Brunei and the western part of North Borneo: British Territories of Borneo, Geological Survey Department, Bulletin (two volumes) 3, 360 p.

Macpherson, C.G., and Hall, R., 2002, Timing and tectonic controls on magmatism and ore generation in an evolving orogen: Evidence from Southeast Asia and the western Pacific, *in* Blundell, D.J., Neubauer, F., and von Quadt, A., eds., The Timing and Location of Major Ore Deposits in an Evolving Orogen: Geological Society of London, Special Publication 204, p. 49–67.

Maffione, M., van Hinsbergen, D.J.J., Koornneef, L.M.T., Guilmette, C., Hodges, K., Borneman, N., Huang, W., Ding, L., and Kapp, P., 2015, Forearc hyperextension dismembered the south Tibetan ophiolites: Geology, v. 43, p. 475–478, https://doi.org/10.1130/G36472.1.

Metcalfe, I., 2011, Tectonic framework and Phanerozoic evolution of Sundaland: Gondwana Research, v. 19, no. 1, p. 3–21, https://doi.org/10.1016/j.gr.2010.02.016.

Metcalfe, I., and Irving, E., 1990, Allochthonous terrane processes in Southeast Asia [and discussion]: Philosophical Transactions of the Royal Society of London. Series A, Mathematical and Physical Sciences, v. 331, p. 625–640.

McCarthy, A., Chelle-Michou, C., Müntener, O., Arculus, R., and Blundy, J., 2018, Subduction initiation without magmatism: The case of the missing Alpine magmatic arc: Geology, v. 46, no. 12, https://doi.org/10.1130/G45366.1.

Meunier, A., Velde, B., and Zalba, P., 2004, Illite K-Ar dating and crystal growth processes in diagenetic environments: A critical review: Terra Nova, v. 16, p. 296–304, https://doi.org/10.1111/j.1365-3121.2004.00563.x.

Milroy, W.V., 1953, Geology of West Sarawak with Notes on the Palaeontology of West Sarawak by W.E. Crews: Sarawak Shell Oilfields Ltd., Report GR602.

Morley, R.J., 1998, Palynological evidence for Tertiary plant dispersals in the SE Asian region in relation to plate tectonics and climate, *in* Hall, R., and Holloway, J.D., eds., Biogeography and Geological Evolution of SE Asia: Leiden, The Netherlands, Backhuys Publishers, p. 211–234.

Moss, S.J., 1998, Embaluh Group turbidites in Kalimantan: Evolution of a remnant oceanic basin in Borneo during the Late Cretaceous to Palaeogene: Journal of the Geological Society, v. 155, p. 509–524, https://doi.org/10.1144/gsjgs.155.3.0509.

Moss, S.J., Carter, A., Baker, S., and Hurford, A.J., 1998, A Late Oligocene tectono-volcanic event in East Kalimantan and the implications for tectonics and sedimentation in Borneo: Journal of the Geological Society, v. 155, p. 177–192, https://doi.org/10.1144/gsjgs.155.1.0177.

Mullin, J.W., 1961, Crystallization: Oxford, UK, Butterworth-Heinemann.

Nagao, K., and Itaya, T., 1988, K-Ar age determination [in Japanese with English abstract]: Memoir of Geological Society of Japan, v. 29, p. 5–21.

Nagao, K., Nishido, H., Itaya, T., and Ogata, K., 1984, An age determination by K-Ar method: Bulletin of the Hiruzen Research Institute, Okayama [in Japanese with English abstract]: Universitas Scientiarum, v. 9, p. 19–38.

Ohmori, K., Taira, A., Tokuyama, H., Sakaguchi, A., Okamura, M., and Aihara, A., 1997, Paleothermal structure of the Shimanto accretionary prism, Shikoku, Japan: Role of an out-of-sequence thrust: Geology, v. 25, p. 327–330, https://doi.org/10.1130/0091-7613(1997)025<0327:PSOTSA>2.3.CO;2.

Orange, D.L., and Underwood, M.B., 1995, Patterns of thermal maturity as diagnostic criteria for interpretation of mélanges: Geology, v. 23, p. 1144–1148, https://doi.org/10.1130/0091-7613(1995)023<1144:POTMAD>2.3.CO;2.

Pevear, D.R., 1992, Illite age analysis, a new tool for basin thermal history analysis, *in* Kharaka, Y.K., and Maest, A.S., eds., Water-Rock Interaction: Moderate and High Temperature Environments: Proceedings of the 7th International Symposium on Water-Rock Interaction, Park City, Utah, USA, 13–18 July: Rotterdam, The Netherlands, A. A. Balkema, v. 2, p. 1251–1254.

Pevear, D.R., 1999, Illite and hydrocarbon exploration: Proceedings of the National Academy of Sciences of the United States of America, v. 96, p. 3440–3446, https://doi.org/10.1073/pnas.96.7.3440.

Raimbourg, H., Famin, V., Palazzin, G., Yamaguchi, A., Augier, R., Kitamura, Y., and Sakaguchi, A., 2019, Distributed deformation along the subduction plate interface: The role of tectonic mélanges: Lithos, v. 334–335, p. 69–87, https://doi.org/10.1016/j.lithos.2019.01.033.

Raymond, L.A., 2019, Perspectives on the roles of melanges in subduction accretionary complexes: A review: Gondwana Research, v. 74, p. 68–89, https://doi.org/10.1016/j.gr.2019.03.005.

Reynolds, R., 1963, Potassium-rubidium ratios and polymorphism in illites and microclines from the clay size fractions of Proterozoic carbonate rocks: Geochimica et Cosmochimica Acta, v. 27, p. 1097–1112, https://doi.org/10.1016/0016-7037(63)90092-9.

Reynolds, R.C., 1993, WILDFIRE©: A Computer Program for the Calculation of Three-dimensional Powder X-ray Diffraction Patterns for Mica Polytypes and Their Disordered Variations: Hanover, New Hampshire, USA, Robert C. Reynolds, 38 p.

Schmidtke, E.A., Fuller, M., and Haston, R.B., 1990, Paleomagnetic data from Sarawak, Malaysian Borneo and the Late Mesozoic and Cenozoic tectonics of Sundaland: Tectonics, v. 9, p. 123–140, https://doi.org/10.1029/TC009i001p00123.

Song, Y., Chung, D., Choi, S., Kang, I., Park, C., Itaya, T., and Yi, K., 2014, K-Ar illite dating to constrain multiple events in shallow crustal rocks: Implications for the late Phanerozoic evolution of NE Asia: Journal of Asian Earth Sciences, v. 95, p. 313–322, https://doi.org/10.1016/j.jseaes.2014.05.018.

Srodon, J., and Eberl, D.D., 1984, Illite: Reviews in Mineralogy, v. 13, p. 495–544.

Steiger, R., and Jäger, E., 1977, Subcommission on geochronology: convention on the use of decay constants in geo- and cosmochronology: Earth and Planetary Science Letters, v. 36, p. 359–362, https://doi.org/10.1016/0012-821X(77)90060-7.

Stern, R.J., Reagan, M., Ishizuka, O., Ohara, Y., and Whattam, S., 2012, To understand subduction initiation, study forearc crust: To understand forearc crust, study ophiolites: Lithosphere, v. 4, p. 469–483, https://doi.org/10.1130/L183.1.

Süssenberger, A., Wemmer, K., and Schmidt, S.T., 2018, The zone of incipient $^{40}Ar^{*}$ loss-monitoring $^{40}Ar^{*}$ degassing behavior in a contact metamorphic setting: Applied Clay Science, v. 165, p. 52–63, https://doi.org/10.1016/j.clay.2018.07.040.

Tan, D.N.K., 1979, Lupar Valley, West Sarawak: Geological Survey of Malaysia, Report 13.

Tan, D.N.K., 1982, Lubok Antu Mélange, Lupar Valley, West Sarawak: A Lower Tertiary subduction complex: Bulletin of the Geological Society of Malaysia, v. 15, p. 31–46, https://doi.org/10.7186/bgsm15198204.

Tan, D.N.K., 1984, Palaeocurrents in the Tertiary sedimentary deposits in western Sarawak: Bulletin of the Geological Society of Malaysia, v. 17, p. 258–264, https://doi.org/10.7186/bgsm17198413.

Tartaglia, G., Viola, G., van der Lelij, R., Scheiber, T., Ceccato, A., and Schnenberger, J., 2020, "brittle structural facies" analysis: A diagnostic method to unravel and date multiple slip events of long-lived faults: Earth and Planetary Science Letters, v. 545, no. 116420, https://doi.org/10.1016/j.epsl.2020.116420.

Tate, R.B., 2002, Geological Map of Borneo: Persatuan Geologi Malaysia: Geological Society of Malaysia, scale 1:1,500,000.

Tonai, S., Ito, S., Hashimoto, Y., Tamura, H., and Tomioka, N., 2016, Complete ^{40}Ar resetting in an ultracataclasite by reactivation of a fossil seismogenic fault along the subducting plate interface in the Mugi Mélange of the Shimanto accretionary complex, southwest Japan: Journal of Structural Geology, v. 89, p. 19–29, https://doi. rg/10.1016/j.jsg.2016.05.004.

Torgersen, E., Viola, G., Zwingmann, H., and Harris, C., 2014, Structural and temporal evolution of a reactivated brittle-ductile fault, Part II: Timing of fault initiation and reactivation by K-Ar dating of synkinematic illite/muscovite: Earth and Planetary Science Letters, v. 407, p. 221–233, https://doi.org/10.1016/j.epsl.2014.09.031.

van der Pluijm, B.A., Hall, C.M., Vrolijk, P.J., Pevear, D.R., and Covey, M.C., 2001, The dating of shallow faults in the Earth's crust: Nature, v. 412, p. 172–175, https://doi. rg/10.1038/35084053.

van der Pluijm, B.A., Vrolijk, P.J., Pevear, D.R., Hall, C.M., and Solum, J., 2006, Fault dating in the Canadian Rocky Mountains: Evidence for Late Cretaceous and early Eocene orogenic pulses: Geology, v. 34, p. 837–840, https://doi.org/10.1130/G22610.1.

Velde, B., and Hower, J., 1963, Petrological significance of illite polymorphism in Paleozoic sedimentary rocks: The American Mineralogist, v. 48, p. 1239–1254.

Verdel, C., van der Pluijm, B.A., and Niemi, N., 2012, Variation of illite/muscovite $^{40}Ar/^{39}Ar$ age spectra during progressive low-grade metamorphism: An example from the US Cordillera: Contributions to Mineralogy and Petrology, v. 164, p. 521–536, https://doi.org/10.1007/s00410-012-0751-7.

Viola, G., Scheiber, T., Fredin, O., Zwingmann, H., Margreth, A., and Knies, J., 2016, Deconvoluting complex structural histories archived in brittle fault zones: Nature Communications, v. 7, no. 13448, https://doi.org/10.1038/ncomms13448.

Vrolijk, P., and van der Pluijm, B.A., 1999, Clay gouge: Journal of Structural Geology, v. 21, p. 1039–1048, https://doi.org/10.1016/S0191-8141(99)00103-0.

Vrolijk, P., David, P., Michael, C., and Allan, L.R., 2018, Fault gouge dating: History and evolution: Clay Minerals, v. 53, p. 305–324, https://doi.org/10.1180/clm.2018.22.

Wakita, K., 2015, OPS mélange: A new term for mélanges of convergent margins of the world: International Geology Review, v. 57, no. 5–8, p. 529–539, https://doi.org/10.1080/00206814.2014.949312.

Wang, P.C., Li, S.Z., Guo, L.L., Jiang, S.H., Somerville, I.D., Zhao, S.J., Zhu, B.D., Chen, J., Dai, L.M., Suo, Y.H., and Han, B., 2016, Mesozoic and Cenozoic accretionary orogenic processes in Borneo and their mechanisms: Geological Journal, v. 51, p. 464–489, https://doi.org/10.1002/gj.2835.

Wilkinson, M., Haszeldine, R.S., and Fallick, A.E., 2014, Authigenic illite within northern and central North Sea oilfield sandstones: Evidence for post-growth alteration: Clay Minerals, v. 49, p. 229–246, https://doi.org/10.1180/claymin.2014.049.2.06.

Williams, P.R., Supriatna, S., and Harahap, B., 1986, Cretaceous mélange in West Kalimantan and its tectonic implications: Geological Survey of Malaysia Bulletin, v. 19, p. 69–78, https://doi.org/10.7186/bgsm19198606.

Williams, P.R., Johnston, C.R., Almond, R.A., and Simamora, W.H., 1988, Late Cretaceous to early Tertiary structural elements of West Kalimantan: Tectonophysics, v. 148, p. 279–297, https://doi.org/10.1016/0040-1951(88)90135-7.

Wolfenden, E.B., 1960, The geology and mineral resources of the lower Rajang Valley and adjoining areas, Sarawak: British Territories Borneo Region Geological Survey Department, Memoir 11, 167 p.

Xiong, Q., Griffin, W.L., Zheng, J.P., O'Reilly, S.Y., Pearson, N.J., Xu, B., and Belousova, E.A., 2016, Southward trench migration at ~130–120 Ma caused accretion of the Neo-Tethyan forearc lithosphere in Tibetan ophiolites: Earth and Planetary Science Letters, v. 438, p. 57–65, https://doi.org/10.1016/j.epsl.2016.01.014.

Yagi, K., Okada, T., Honjou, Y., and Itaya, T., 2015, Argon analyses by isotopic dilution method using argon 38 spike with HIRU: Reproducibility and reliability in 25 years K-Ar dating: Bulletin of the Research Institute of Technology, Okayama: Universitas Scientiarum, v. 33, p. 42–52.

Yang, J.F., Lu, G., Liu, T., Li, Y., Wang, K., Wang, X.X., Sun, B.L., Faccenda, M., and Zhao, L., 2020, Amagmatic subduction produced by mantle serpentinization and oceanic crust delamination: Geophysical Research Letters, v. 47, no. 9, https://doi.org/10.1029/2019GL086257.

Zhao, M.W., Ahrendt, H., and Wemmer, K., 1997, K-Ar systematics of illite/smectite in argillaceous rocks from the Ordos basin, China: Chemical Geology, v. 136, p. 153–169, https://doi.org/10.1016/S0009-2541(96)00132-5.

Zwingmann, H., and Mancktelow, N.S., 2004, Timing of Alpine fault gouges: Earth and Planetary Science Letters, v. 223, p. 415–425, https://doi.org/10.1016/j. psl.2004.04.041.

Zwingmann, H., Offler, R., Wilson, T., and Cox, S., 2004, K-Ar dating of fault gouge in the northern Sydney basin, Australia: Implications for the breakup of Gondwana: Journal of Structural Geology, v. 26, p. 2285–2295, https://doi.org/10.1016/j.jsg.2004.03.007.

Zwingmann, H., Den Hartog, S.A.M., and Todd, A., 2019, The effect of sub-seismic fault slip processes on the isotopic signature of clay minerals: Implications for K-Ar dating of fault zones: Chemical Geology, v. 514, p. 112–121, https://doi.org/10.1016/j.chemgeo.2019.03.034.

Science Editor: Brad S. Singer
Associate Editor: William Guenthner

Manuscript Received 8 September 2020
Revised Manuscript Received 2 February 2021
Manuscript Accepted 17 March 2021

Printed in the USA